Francisco Manuel de Carvalho Simões

Licenciatura em Biologia Celular e Molecular

Cavin 1 and Cavin 2 Roles on Adipocyte Cell Function

Dissertação para obtenção do Grau de Mestre em
Genética Molecular e Biomedicina

Orientador: Marta Camps, Prof.Doutora, FB-UB
Elo de Ligação: Nuno Neves, Prof.Doutor, FCT-UNL

Júri:

Presidente: Prof. Doutor José Paulo Sampaio
Arguente: Prof. Doutora Maria da Graça Tavares Rebelo de Soveral Rodrigues
Vogal: Prof. Doutora Marta Camps Camprubí

FACULDADE DE CIÊNCIAS E TECNOLOGIA
UNIVERSIDADE NOVA DE LISBOA

Dezembro, 2011

Cavin 1 and Cavin 2 Roles on Adipocyte Cell Function

Abstract

Caveolae are a specialized type of lipid rafts found in numerous cell types. These structures have been implicated as playing a role in a variety of metabolic regulation processes and are typically characterized by their association with the caveolin and cavin protein families. Caveolae are particularly enriched in adipocytes and here we analyze the effects of cavin 1 and cavin 2 knockdown in adipocyte functioning. We obtained several multiclonal mouse 3T3-L1 cell lines with reduced expression of cavin 1 or cavin 2 by small interfering RNA approach using lentiviral vectors. We observed that cavin 1, but not cavin 2, depletion affects adipocyte differentiation and that both knockdown cells showed a reduced number of caveolae. We also verified that cavin 1 and cavin 2 expressions levels are dependent on each other and that both knockdowns caused a specific decrease in glucose transporter 4 (GLUT4) protein levels. Besides the lower protein levels of GLUT4, both knockdown cells also fail to translocate the transporter to the plasma membrane in response to insulin, although the insulin signaling pathway was not affected. As a consequence, knockdown cells show reduced insulin-stimulated glucose transport. Our results underscore the importance of cavin 1 and cavin 2 in glucose uptake and adipocyte metabolism.

Keywords: Cavin 1; Cavin 2; GLUT4; Adipocytes;Caveolin-1;Caveolae

Resumo

Caveolas são um subtipo de *lipid rafts* presentes em diversos tipos celulares. Estas estruturas estão envolvidas em diversos processos de regulação metabólica e são tipicamente caracterizadas pela associação às famílias de proteínas, caveolinas e cavinas. As caveolas são particularmente abundantes em adipócitos e neste trabalho analisamos os efeitos do *knockdown* de cavina 1 ou cavina 2 no funcionamento de adipócitos. Foram obtidas várias linhas celulares 3T3-L1 de rato, multiclonais, com reduzida expressão de cavina 1 ou cavina 2, utilizando RNA de interferência e vectores lentivíricos. Observámos que a redução proteica de cavina 1, mas não de cavina 2, afecta a diferenciação adipocitária e que ambos os *knockdowns* provocam uma redução no número de caveolas. Também verificámos que os níveis de expressão de cavina 1 e cavina 2 são interdependentes e que o *knockdown* de cada uma das proteínas causa uma redução proteica do transportador de glucose 4 (GLUT4). Para além dos reduzidos níveis proteicos de GLUT4, ambas as linhas celulares *knockdown* não conseguem enviar este transportador para a membrana plasmática quando estimuladas por insulina, embora a cascata de sinalização por insulina não esteja afectada. Como consequência, as células *knockdown* apresentam um reduzido transporte de glucose em resposta a insulina. Os nossos resultados demonstram a importância de cavina 1 e cavina 2 na captação de glucose e no metabolismo de adipócitos.

Palavras-chave: Cavina 1; Cavina 2; GLUT4; Adipócitos; Caveolina-1; Caveolas

Contents

Index of Figures

Index of Tables

List of abbreviations

Akt/PKB	Protein Kinase B
APS	Ammonium Persulfate
AS160	Akt Substrate of 160 kDa
ATGL	Adipose Triglyceride Lipase
BAT	Brown Adipose Tissue
BSA	Bovine Serum Albumine
CS	Calf Serum
DAG	Diacylglyceride
DMEM	Dulbecco's Modified Eagle Medium 1x
DMSO	Dimethyl Sulfoxide
DTT	Ditriotheitol
ECL	Enhanced Chemiluminescence
EDTA	Ethylenediaminetetraacetic Acid
EGTA	Ethylene Glycol Tetraacetic Acid
FAPB4	Fatty Acid Biding Protein 4
FBS	Fetal Bovine Serum
FFA	Free Fatty Acids
GGA	Golgi-localized, γ-ear-containing, Arf (ADP-ribosylation factor)-binding protein
GLUT1/4	Glucose Transporter Type 1 or 4
GSV	Glucose Transporter Isoform 4 Storage Vesicle
HEPES	4-(2-hydroxyethyl)-1-Piperazineethanesulfonic Acid
HSL	Hormone Sensitive Lipase
IBMX	1-Metil-3-Isobutilxantina
IR	Insulin Receptor
IRS-1	Insulin Receptor Substrate 1
KD	Knockdown
KO	Knockout
LD	Lipid Droplets
LSB	Laemmli Sample Buffer
MAG	Monoacylglyceride
PBS	Phosphate Buffered Saline
PEI	Polyethylenimine
PFA	Paraformaldehyde
PH	Pleckstrin Homology

PI3K	Phosphatidylinositol 3-Kinase
PIP_3	Phosphatidylinositol-3,4,5-triphosphate
PKC ζ	Protein Kinase C Zeta
PKD	Phosphoinositide-Dependent Kinase
PMSF	Phenylmethylsulfonyl Fluoride
PVDF	Polyvinylidene Fluoride
RE	Recycling Endossomes
RIPA	Radioimmunoprecipitation Assay
SDS	Sodium Dodecyl sulfate
SH2	Scr Homology 2
siRNA	Small Interference RNA
T2D	Type 2 Diabetes
TAG	Triacylglyceride
TEMED	Tetramethylethylenediamine
VAMP	Vesicle-Associated Membrane Protein
WAT	White Adipose Tissue

1. Introduction

1.1 Obesity and Type 2 Diabetes

Obesity, defined as an abnormal or excessive fat accumulation that may impair health (World Health Organization, 2011a), is a condition that affects millions of people around the world, specially in western countries where the aggressive promotion of processed food, which commonly have high fat and carbohydrate content, coupled with reduction in caloric expenditure due to sedentary lifestyle is more evident (Friedman, 2002; Unger, 2003; Virally *et al*., 2007).

Complications associated with obesity appear when adipose tissue exceeds its capacity to store lipids which results in deposition of these lipids in non-adipose tissues, such as pancreatic β-cells, liver, cardiac myocytes and skeletal muscle. In contrast to adipocytes, these tissues are poorly adapted to store lipids and this lipid deposition triggers lipotoxic disruption of cellular functions. Lipotoxicity, defined as lipid-induced dysfunction in non-adipose tissue, is of a central importance in the development of metabolic diseases such as Type 2 Diabetes (T2D), atherosclerosis, hypertension, etc (Blouin *et al*., 2008; Campbell, 2009; Costacou and Mayers-Davis, 2003; Friedman, 2002; Le Lay *et al*., 2009).

In the last years, prevalence of T2D increased alarmingly, giving diabetes the dimension of an epidemic disease (Costacou and Mayers-Davis, 2003). The disease comprises a complex and heterogeneous group of metabolic disorders often related with hyperglycemia (excessive hepatic glucose production and/or reduced glucose uptake), obesity and impaired insulin action (Friedman, 2002; Guillausseau *et al*.,2008; Lin and Sun, 2010). Over time, diabetes can damage the heart, blood vessels, eyes, kidneys, and nerves. In the world, 346 million people have diabetes and T2D comprises 90% of the cases (World Health Organization, 2011b) and it has also been estimated that from 1995 to the year 2025, the prevalence of diabetes will increase 42% among adults living in the developed world (Costacou and Mayers-Davis, 2003). Striking parallel increases in the prevalence of obesity reflect the importance of body fatness as a contributing factor to diabetes incidence. It is estimated that the risk of developing T2D is up to 75% in obese individuals (Costacou and Mayers-Davis, 2003; Virally *et al*., 2007).

Improved understanding of the molecular mechanisms behind energy homeostasis might lead to effective strategies for the treatment of obesity and metabolic diseases.

1.2 Adipocytes biology

The adipose tissue is the body's largest energy reservoir and so it is an important metabolic organ, crucial for whole-body insulin sensitivity and energy homeostasis. (Lafontan and Langin, 2009; Le Lay *et al*., 2009; Lefterova and Lazar, 2009; Unger, 2003) There are two types of adipose tissue,

the white adipose tissue (WAT) and brown adipose tissue (BAT). WAT, which is the predominant type of fat in adult humans, serves as a storage depot for excess energy, whereas BAT generates heat in newborns and rodents. (Lefterova and Lazar, 2009)

Most energy reserves in the human body, lipids and glucose, are stored in fat cells as triacylglycerides (TAGs) and the adipose tissue is capable of exerting a buffer activity by increasing plasma TAG clearance and suppressing the release of free fatty acids (FFA) into circulation (Bickel *et al*., 2009; Ducharme and Bickel, 2008; Lafontan and Langin, 2009; Le Lay *et al*., 2009). In adipocytes (figure 1.1), TAGs arise from two major routes: *de novo* lipogenesis from non-lipid precursors (for example glucose) or uptake of FFA from plasma. In situations where energy is required (fasting and physical exercise) these TAGs are broken down to FFA and glycerol in a process called lipolysis (Lafontan and Langin, 2009; Le Lay *et al*., 2009). Glycerol and fatty acids are substracts for gluconeogenesis and ketogenesis, respectively, in liver. Skeletal muscle and heart use fatty acids for energy provision via mitochondrial β-oxidation and generation of ATP (Ducharme and Bickel, 2008).

These metabolic processes (lipogenesis and lipolysis) are controlled by different stimulus being the most relevant, insulin and catecholamines (Bickel *et al*., 2009; Lafontan and Langin, 2009).

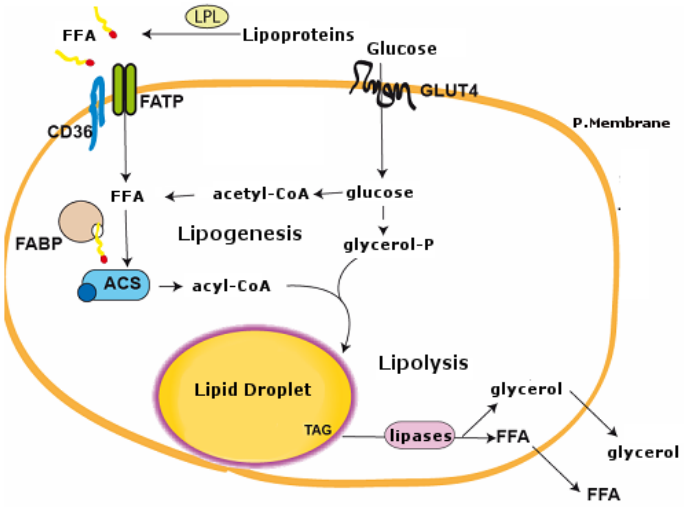

Figure 1.1. Lipid metabolism in adipocytes. Lipogenesis and Lipolysis. FFA: free fatty acids; FABP: Fatty acid binding protein; FATP: Fatty acid transport proteins; CD36: Fatty acid translocase; ACS: Acyl-CoA synthetase; LPL: Lipoprotein lipase; TAG: triacylglyceride. (Adapted from González-Muñoz, 2007).

1.2.1 Lipolysis regulation

Adipocytes possess specialized structures, called Lipid Droplets (LDs), where the TAGs are stored. LDs contain a core of neutral lipids surrounded by a phospholipid monolayer and coated by

specific proteins such as perilipin, a member of the PAT protein family. The protein content of the LDs can vary within droplets of the same cell and between cell types (Bickel *et al*., 2009).

Perilipin was the first member of the termed "PAT family" and in mice and humans a single perilipin gene gives rise to 3 isoforms of the protein (with approximately 55 kDa), by alternative splicing. Perilipin A (56,8 kDa) is the most abundant isoform and the focus of all functional studies (Bickel *et al*., 2009; Brown, 2001; Forcheron *et al*., 2005).

Perilipin has a major role in regulating the accessibility to the TAGs stored in the LDs. This protein can either restrict LD accessibility of enzymes that hydrolyze lipid esters (lipases) or facilitate their enzymatic activity under appropriate metabolic conditions. In adipocytes, in the lipolytic pathway, catecholamines signal through a β-adrenergic receptor and G-protein coupled signaling cascade to elevate cellular cAMP levels. This in turn activates cAMP-dependent Protein Kinase A, which phosphorylates perilipins and hormone sensitive lipase (HSL). HSL then translocates from cytoplasm to the LDs surface and the access to TAG is facilitated by the phosphorylated perilipins. (Lafontan and Langin, 2009; Bickel *et al*., 2009; Ducharme and Bickel, 2008).

Recently another lipase, adipocyte triglyceride lipase (ATGL) has emerged as the major TAG Lipase. ATGL catalyzes the initial step in lipolysis (hydrolysis of TAG to Diacylglyceride, DAG), while HSL catalysis the second step (hydrolysis of DAG to Monoacylglyceride, MAG). Finally a soluble monoglyceride lipase catalyzes the breakdown of MAG to glycerol and FFA. In contrast to HSL, ATGL appears to reside on the LD surface and to be independent of Protein Kinase A activation. Glycerol is used as a gluconeogenic substract in the liver and FFA as a source of energy in the liver, skeletal muscle and heart (Bickel *et al*., 2009; Brown, 2001; Ducharme and Bickel, 2008).

1.3 Insulin action and glucose transport

Adipose tissue plays a critical role in energy homeostasis in higher organisms. It is able to remove glucose and TAGs from plasma and store it inside special structures called LDs and so avoiding fatty acids accumulation in other organs where it could trigger lipotoxic disruption of cellular functions (Blouin *et al*., 2008; Le Lay *et al*., 2009). In both muscle and fat cells, insulin stimulates the translocation of the Glucose Transporter Type 4 (GLUT4) (main glucose transporter in these cells) from an intracellular location to the cell surface, where it facilitates the reduction of plasma glucose levels (Bryant *et al*., 2002).

Understanding the molecular mechanisms that mediate this translocation event involves integrating our knowledge of two fundamental processes — the signal transduction pathways that are triggered when insulin binds to its receptor and the membrane trafficking events that need to be modified to divert GLUT4 from intracellular storage to the plasma membrane.

1.3.1 Insulin biology

Insulin is a peptidic anabolic hormone, composed of 51 a.a. and with a molecular weight of 5808Da. It is a small protein made of two polypeptide chains and exerts its function through biding to its receptors located in many cell types. Insulin is produced in β-pancreatic cells and has a central role in cellular metabolism and in lowering blood glucose concentration (Aronoff *et al*., 2004).

In order to reduce the glucose concentration in the blood, insulin-sensitive tissues, like adipose tissue and skeletal muscle, increase glucose uptake upon insulin binding through recruitment of GLUT4 to the plasma membrane. Insulin also inhibits pancreatic α-cells glucagon production, which leads to the inhibition of hepatic gluconeogenesis and glycogenolysis (Aronoff *et al*., 2004; González-Muñoz, 2007; Klip, 2009; Young, 2005).

Insulin is also important in the cellular metabolism of adipocytes. It promotes adipocytes differentiation, uptake not only of glucose but also of FFA, lipoprotein lipase activity, synthesis of TAG from both glucose (de novo lipogenesis) and from FFA (lipogenesis) and inhibition of lipolysis of TAGs stored in LD (González-Muñoz, 2007).

The failure of insulin to stimulate glucose uptake and storage appears to be a primary defect already detectable at the initial stages of insulin resistance (DeFronzo and Tripathy, 2009; Lamb *et al*., 2010; Vollenweider *et al*., 2002).

1.3.2 Insulin signaling pathway

The most accepted insulin signaling pathway that leads to the translocation of GLUT4 to the membrane is the Phosphatidylinositol 3-Kinase (PI3K) dependent pathway (figure 1.2) (Farese, 2002; Welsh *et al.*, 2005). This insulin pathway involves a cascade of events initiated by insulin binding to its cell surface receptor (IR). Following insulin biding to IR it becomes activated by autophosphorylation and phosphorylates tyrosines in the Insulin Receptor Substrate 1 (IRS-1). The tyrosines act as a docking site for the Scr Homology 2 (SH2) domain that exists in the p85 subunit of PI3K and IRS-1 activates PI3K. Following PI3K activation there is a production of lipidic second messengers, like Phosphatidylinositol-3,4,5-triphosphate (PIP_3), which leads to the stimulation of downstream proteins including Protein Kinase B (PKB or Akt) and Protein Kinase C Zeta (PKC ζ). Akt phosphorylates the Rab GTPase activating protein (Akt Substrate 160kDa (AS160)), which in turn is inhibited, allowing the stabilization of Rab proteins that together with PKC ζ lead to the translocation of GLUT4 from intracellular vesicles to the plasma membrane (Choi and Kim, 2010; González-Muñoz, 2007; Rowland *et al.*, 2011; Watson and Pessin, 2006).

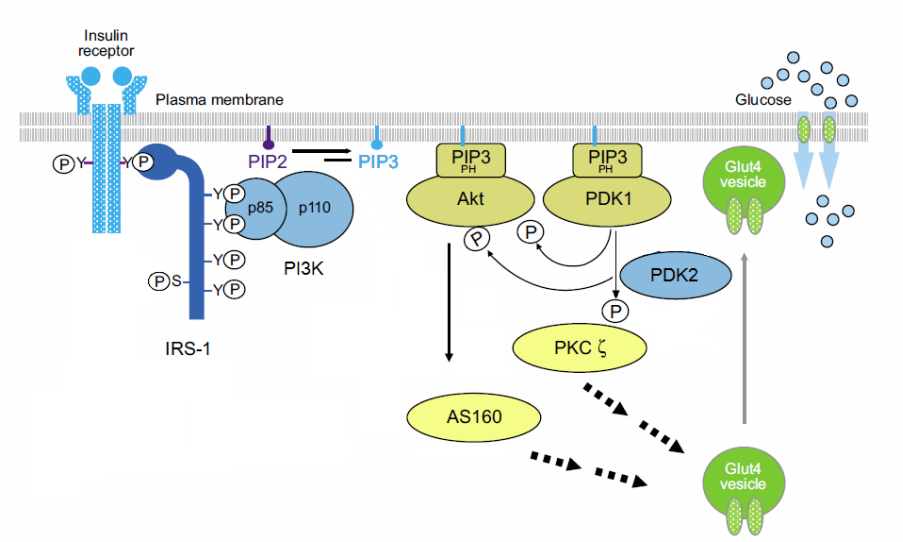

Figure 1.2. The insulin signaling pathway. Akt: protein kinase B; AS160: Akt 160KDa substrate; GLUT4: glucose transporter 4; IRS-1: insulin receptor substrate-1; PDK: phosphoinositide-dependent kinase; PKC ζ: protein kinase C zeta; PH: pleckstrin homology domain; PI3K: phosphoinositide 3-kinase (regulatory subunit p85 and catalytic subunit p110); PIP: phosphatidylinositol phosphate. (Adapted from Choi and Kim, 2010).

1.3.2.1 Insulin receptor

The IR belongs to a family of cell-surface receptors that possess intrinsic tyrosine kinase activity (Huang and Chen, 2009). IR is composed of two extracellular α and two transmembrane β subunits disulfide-linked into an $\alpha_2\beta_2$ heterotetrameric structures (González-Muñoz, 2007; Watson and Pessin, 2001). Upon insulin binding to the α-subunits, a transmembrane conformational change is generated that activates the intracellular subunit tyrosine kinase domain. The β-subunit undergoes a series of intramolecular autophosphorylations, activating them. After this, IR is able to phosphorylate the subsequent insulin signaling cascade proteins like the IRS-1 (Choi and Kim, 2010; González-Muñoz, 2007; Watson and Pessin, 2001; Zaid *et al*., 2008).

1.3.2.2 Insulin Receptor Subtract

IRS-1 is a key mediator in the insulin signaling cascade. IRS family members contain a NH_2-terminal Pleckstrin Homology (PH) domain that binds to membrane phospholipids, an adjacent phosphotyrosine-binding domain and a variable length C-terminal tail that contains a number of tyrosine and serine phosphorylation sites (Boura-Halfon and Zick, 2009; Zaid *et al*., 2008). Several of these phosphorylation sites are located in amino acid sequence motifs that bind to SH2 domain proteins (Sesti et al., 2001; Zaid *et al*., 2008).

1.3.2.3 Phosphatidylinositol 3-kinase

PI3K is a heterodimeric lipid kinase, with a regulatory (85KDa) and a catalytic subunit (110KDa), with four isoforms (α, β, γ and δ), according to catalytic subunit differences, and plays an essential role in glucose uptake and GLUT4 translocation (González-Muñoz, 2007; Huang and Chen, 2009; Zaid et al., 2008).

In a basal situation (without insulin) PI3K is in the cytosol, in the presence of insulin the p85 subunit interacts with phosphorylated IRS-1 through SH2 domain (present in p85 subunit) and brings p110 subunit closer to the membrane. This proximity allows p110 to phosphorylate membrane phospholipids and Phosphatidylinositol 4,5-biphosphate on the 3' position, catalyzing the formation of PIP_3. PIP_3 is able to stimulate the activity of Phosphoinositide-Dependent Kinases (PKD-1 and PKD-2) which initiates the activation of its downstream effectors, Akt and PKC ζ (González-Muñoz, 2007; Choi and Kim, 2010; Watson and Pessin, 2001).

1.3.2.4 Akt (or PKB)

The serine/threonine protein kinase Akt plays important roles in several signaling cascades (Liao and Hung, 2010). Akt has 3 different isoforms, Akt1/PKBα, Akt2/PKBβ and Akt3/PKBγ, which have distinct tasks in cell survival, growth and metabolism (Bellacosa *et al.*, 2004). Akt2 is primarily important for glucose homeostasis by being a signaling molecule in the insulin signaling cascade.

Each Akt isoform possess an N-terminal PH domain, which allows Akt to bind PIP_3, a C-terminal regulatory domain containing a hydrophobic motif and a central kinase domain (Bellacosa *et al.*, 2004). Akt is able to bind to the PI3K products (PIP_3) and this union has a double action. First it moves Akt from the cytosol to the membrane, closer to both PKDs, second it induces conformational changes in Akt that make its phosphorylation by PKD-1 (Thr308) and PKD-2 (Ser473) possible (Choi and Kim, 2010;Rowland *et al.*, 2011; Watson and Pessin, 2001). When phosphorylated, Akt is fully activated.

1.3.2.5 Protein Kinase C zeta

PKC ζ is a member of the PKC serine-threonine family, that acts downstream of PI3K. The PKC family plays important roles in many intracellular signaling events, cell growth and differentiation (Sampson and Cooper, 2006).

In the absence of insulin, PKC ζ was described to be a negative regulator of Akt (Dandekar et al., 1998; Doornbos et al., 1999) while in the presence of insulin, PKC ζ becomes activated and enables Akt activity and GLUT4 translocation. Not only insulin but also glucose and exercise can

activate PKC ζ through diverse pathways. For that, PKC ζ activation and activity are impaired in insulin resistance in muscle and adipose tissues of type II diabetic individuals (Liu *et al.,* 2006).

1.3.3 GLUT4

Facilitated glucose transporters family is characterized by 12 transmembrane domains that allow all the isoforms to catalyze hexose transport across the cell through an ATP-independent facilitative diffusion mechanism (Huang and Czech, 2007).

Adipocytes express Glucose Transporter Type 1 (GLUT1) and GLUT4. GLUT1 presents a ubiquitous expression and is responsible for the basal glucose transport in these cells. GLUT4 is responsible for the insulin-stimulated glucose transport in adipocytes, skeletal muscle and heart (González-Muñoz, 2007; Watson and Pessin, 2001).

In contrast to the other GLUT isoforms, which are primarily localized to the plasma membrane in the absence of insulin, GLUT4 transporter proteins are retained into specialized storage vesicles connected to the endosomal-trans Golgi network system, called Glucose Transporter Isoform 4 Storage Vesicle (GSVs) (Klip, 2009; Lamb *et al.*, 2010; Watson *et al.*, 2004; Williams *et al.*, 2006; Zaid *et al.*, 2008).

In unstimulated muscle or adipocytes (absence of insulin), 4-10% of GLUT4 is located at the cell surface and >90% at intracellular compartments (GSVs). This steady-state distribution of GLUT4 is the balance of its fast endocytosis and slow exocytosis (Bryant, 2002; Lamb, 2007; Zaid *et al.*, 2008).

In the presence of insulin, the hormone initiates the insulin-signaling cascade which leads to the accumulation of GLUT4 at the plasma membrane (approximately 55% in specialized structures called caveolae) (Ros-Baró *et al*., 2001; Karlsson *et al*., 2002) by increasing exocytosis and modestly decreasing the endocytosis rate of the GSVs (Bryant *et al.*, 2002; Klip, 2009; Zaid *et al.*, 2008).

So that the increase in exocytosis occurs it is necessary that the substrate of Akt, the AS160 is phosphorylated. AS160 is phosphorylated and inhibited both Akt, and is involved in the regulation of several membrane transport steps, including vesicle budding, motility, tethering and fusion (Choi and Kim, 2010; González-Muñoz, 2007; Rowland *et al.*, 2011; Watson and Pessin, 2006). The consequence of such inhibition is the stabilization of the AS160 target Rab proteins in the GTP-bound form, which is thought to promote vesicle trafficking (Klip, 2009; Rowland *et al.*, 2011; Watson and Pessin, 2006).

1.4 Caveolae

Lipid rafts are lateral assemblies of sphingolipids and cholesterol that form a separate liquid-ordered phase in the liquid disordered matrix of the lipid bilayer. Lipid rafts function as platforms with which distinct classes of proteins are associated, such as glycosylphosphatidylinositol-anchored

proteins, transmembrane proteins, and diacylated proteins (Lajoie and Nabi, 2010; Ros-Baró *et al*., 2001).

Caveolae, morphologically described in the early 1950s, are a specialized type of lipid raft that appear in the plasma membrane (Briand *et al.*, 2010; González-Muñoz *et al*., 2009; Parton *et al*., 2006). These membrane strutures were first identified by electron microscopy and were defined as flask-shaped invaginations with 50-100nm of diameter (Chadda and Mayor, 2008; Hansen and Nichols, 2010; Liu *et al*., 2008). Caveolae function has been widely debated and has been implicated in membrane trafficking, signal transduction, substrate transport, endocytosis and cancer (Briand *et al*., 2010; Hayer *et al*., 2010; Hansen and Nichols, 2010). These structures have also been exploited by pathogens, both as direct portals for endocytic entry and to facilitate the entry of pathogens that are larger than a single caveolae (Parton and Simons, 2007). Caveolae are present in many cell types like muscle cells, endothelian cells, but are particularly abundant in adipocytes, where they account for 30% of the plasma membrane surface and recently caveolae were defined as indispensable structures in the protection of fat cells against lipotoxic effects of elevated levels of fatty acids (Meshulam *et al*., 2011).

IR and GLUT4 are two important molecules in the mechanism of removing glucose from blood in response to insulin, as described in section 1.3. In adipocytes IR and GLUT4, when in the membrane, are localized in caveolae and it has been shown that in the absence of these structures, the levels of IR and GLUT4 are decreased (González-Muñoz *et al*., 2009; Meshulam *et al.,*2011). Thereby caveolar formation and stability is critical to the adipocytes metabolism. Caveolae have two major protein components, caveolins and cavins (González-Muñoz *et al*., 2009).

1.4.1 Caveolins

Caveolins are the major coat constituent of caveolae. Caveolins family comprises caveolin-1, the main and most widespread caveolin, caveolin-2, expressed in the same cells that caveolin-1, and caveolin-3 expressed exclusively in muscle cells (Hansen and Nichols, 2010; Hill *et al*., 2008; Parton *et al*., 2006). The 3 isoforms have molecular weights between 15 and 20 kDa and all of them are multiply acylated proteins embedded in the cytosolic leaflet of cell membrane (never reaching the outside of the cell), with both N- and C-termini residing in the cytosol (figure 1.3) (González-Muñoz, 2007; Hansen and Nichols, 2010; Liu and Pilch, 2008).

Caveolins are able to form oligomers and act as scaffolding proteins that bind and concentrate cholesterol. It is estimated that caveolin-1 forms oligomers of 14-16 monomers and that each caveolae has around 144 caveolin molecules (González-Muñoz, 2007; Hansen and Nichols, 2010; Hill *et al*., 2008). In addition to their structural role, caveolins are also involved in endocytosis/transcytosis and cholesterol/lipid trafficking. Moreover, caveolins can also segregate signal initiation events by concentrating and organizing signaling molecules (González-Muñoz *et al*., 2009; Hansen and Nichols,

2010; Hill *et al*., 2008). Besides its presence and role within caveolae, caveolin-1 has also been identified in LDs (Blouin *et al*., 2008). Although its role in LDs is unclear, it has been observed that caveolin-1 concentration on adipocyte LD positively correlated with LD size in obese rodent models and human adipocytes (Blouin *et al*., 2010). Moreover caveolin-1 null mice exhibit markedly attenuated lipolytic activity (Cohen *et al*., 2004; Meshulam *et al.,*2011). Caveolins have also been strongly linked to breast and prostate cancer (Engelman *et al*., 1998; Tahir *et al*., 2008) and, in the case of muscle-specific caveolin-3, to muscle diseases known as muscular caveolinopathies (Bastiani *et al*., 2009).

Caveolin-1 expression, and caveolin-3 in muscle cells, is necessary for caveolae formation (Hayer *et al*., 2010; Liu *et al*., 2008; Parton *et al*., 2006). It has been shown that the lack of caveolin-1 and caveolin-3 results in absence of caveolae and that these structures are restored upon caveolin-1 or -3 expression (Hansen and Nichols, 2010). By contrast, loss of caveolin-2, which is generally expressed together with caveolin-1, does not affect the formation of caveolae (Hansen and Nichols, 2010; Hayer *et al*., 2010; Parton *et al*., 2006).

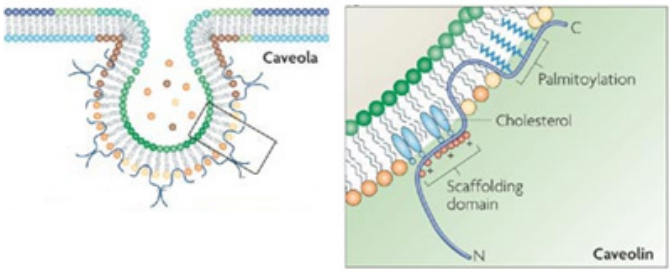

Figure 1.3. Caveolin-1structure and disposition in caveolae. Caveolin is inserted into the caveolar membrane, with the N and C termini facing the cytoplasm and a putative 'hairpin' intramembrane domain embedded within the membrane bilayer. The scaffolding domain, a highly conserved region of caveolin, might have a role in cholesterol interactions through conserved basic (+) and bulky hydrophobic residues (red circles). The C-terminal domain, contains three cysteine residues modified by palmitoyl groups. (Adapted from Parton and Simons, 2007)

1.4.2 Cavins

Cavins are another essential caveolae component (figure 1.4) (Hansen and Nichols, 2010; Hill *et al*., 2008; Liu *et al*., 2008). This family comprises 4 isoforms, polymerase I and transcript release factor (PTRF or cavin 1); serum deprivation protein response (SDPR, SDR or cavin 2); SDR related gene product that binds to protein C-kinase (SRBC or cavin 3) and muscle restricted coiled-coil protein (MURC or cavin 4) (Briand *et al*., 2010; Hayer *et al*., 2010).

Cavin 1 to 3 family members display the same pattern of expression as caveolin-1whereas cavin 4 expression parallels that of caveolin-3 (Bastiani *et al*., 2009; Liu *et al*., 2008). All of them

have been shown to be present in caveolae and to show similar features in terms of molecular organization (Briand *et al*., 2010; Hansen and Nichols, 2010). Indeed, they all contain putative leucine zippers-like domains normally involved in protein-protein interations and, excepting cavin 4, PEST domains (regions rich in proline (P), glutamic acid (E), serine (S), and threonine (T)). Another common feature between cavins is their ability to bind phosphatidylserine and to be phosphorylated in multiple sites (Briand *et al*., 2010; Hayer *et al*., 2010).

Several studies have shown that an important aspect of the biology of cavins is their ability to form complexes with each other (cavins can form complexes even in the absence of caveolin proteins) (Briand *et al*., 2010; Hayer *et al*., 2010). The fact that cavins show tissue-specific expression profiles implies that the cavin complexes associated with caveolae are different in different tissues and the stoichiometry between cavins could determine the functionality of caveolae (Bastiani *et al*., 2009; Briand *et al*., 2010; Nabi, 2009). Therefore, cavins are of extreme importance in the correct function of caveolae.

1.4.2.1 Cavin 1

Cavin 1 was originally identified as a soluble nuclear factor that regulates transcription, it was only recently that this factor was abundantly found in the cytoplasmic face of caveolae, leading cavin 1 to be consider a caveolae marker (Briand *et al*., 2010; Hill *et al*., 2008; Vinten *et al*., 2005).

Cavin 1 is located to caveolae in both muscle and non-muscle tissues, having in this manner a tissue distribution broader than that of either caveolin-1 or caveolin-3 (Hansen and Nichols, 2010). In non-muscle tissues, cavin 1 expression was found to be strictly parallel to that of caveolin-1, it is estimated that cavin 1 and caveolin-1 are present in a 1:1 ration within caveolae (Chadda and Mayor, 2008; Hill *et al*., 2008).

Previous experiments revealed that cavin 1 downregulation results in a reduction of cavin 2 and cavin 3 expression levels and in an increase of caveolin-1 mobility, which is released from the cell surface and rapidly internalized and degraded (Bastiani *et al*., 2009; Chadda and Mayor, 2008; Hill *et al*., 2008), as a result the absence of cavin 1 leads to the loss of morphologically identifiable caveolae (Briand *et al*., 2010; Hill *et al*., 2008; Nabi, 2009). Moreover experimental results tend to prove that cavin 1 is specially important to the last steps of caveolae biogenesis (figure 1.4) (Chadda and Mayor, 2008; Hill *et al*., 2008; Liu and Pilch, 2008). Indeed, cavin1 only associates with plasma membrane caveolin but not with non-caveolar caveolins (like caveolins at the Golgi apparatus) (Hansen and Nichols, 2010; Hayer *et al*., 2010). Therefore, cavin 1 has to be considered as a soluble protein which would be recruited to caveolae, operating like a new scaffold stabilizing the caveolae unit (Briand *et al*., 2010). Not only cavin 1 is necessary for caveolae formation but it has also been suggested that cavin 1 is required to recruit cavin complexes to caveolae (Bastiani *et al*., 2009). Besides caveolae localization, cavin 1 has also been found in the membrane of LDs in association with caveolin-1 and to

be implicated in lipolysis regulation together with HSL (Aboulaich *et al*., 2006). It has also been demonstrated that mice lacking cavin 1 present a higher circulating TAG levels, reduced adipose tissue, glucose intolerance, hyperinsulinemia, all consistent with a lipodystrophic phenotype (Liu *et al*., 2008)

1.4.2.2 Cavin 2

Cavin 2 shares more than 20% similarities with cavin 1 (Briand, 2010; Hansen, 2009). This second member of the cavin family was found to be enriched in caveolae and to co-localize with caveolin-1 and cavin 1 (Briand, 2010; Hansen *et al*., 2009; Hansen and Nichols, 2010). It has been shown that cavin 2 is able to bind cavin 1, independently of caveolin-1, and recruit it to caveolae (Briand *et al*., 2010; Hansen *et al*., 2009). Experimental results have shown that cavin 2 downregulation induces loss of cavin 1 and caveolin-1 expression and therefore limits caveolae formation and even if caveolin-1 and cavin 1 are overexpressed, cavin 2 downregulation still reduces caveolae formation (Briand, 2010; Hansen *et al*., 2009; Hansen and Nichols, 2010; Nabi, 2009). Thereby, cavin 1, cavin 2 and caveolin-1 are functionally interdependent. An interesting observations is that, unlike cavin 1 and caveolin-1, overexpression of cavin 2 alone does not increase caveolae number instead induces changes in caveolae morphology, which turns to appear larger and induces caveolae-associated tubule formation (Briand *et al*., 2010; Hansen *et al*., 2009; Nabi, 2009). Therefore, cavin 2 could be seen as the membrane curvature-inducing component of caveolae (figure 1.4).

1.4.2.3 Cavin 3

Considering its homology with cavin 1, a role in caveolae structure has been considered, however it is still not clear whether cavin 3 is directly required for caveolae morphogenesis or not (Hansen and Nichols, 2010), but it has been shown that cavin 3 associates with caveolin-1 and that it is able to regulate caveolae endocytosis (figure 1.4) (Hayer *et al*., 2010; Nabi, 2009). In contrast with cavin 1 and cavin 2, cavin 3 knockdown (KD) does not affect caveolin-1 levels, however it limits budding and intracellular trafficking of caveolin-1-positive vesicles from the plasma membrane (Briand *et al*., 2010; McMahon *et al.*, 2009; Nabi, 2009).

Apart from the role in adipocytes, it has been shown that the human CAVIN3 gene is situated in a tumor suppressor region and is inactivated in breast and lung cancer (Briand *et al*., 2010).

1.4.2.4 Cavin 4

Cavin 4 is a muscle-specific protein (expression pattern parallels that of caveolin-3), previously described as purely cytosolic and able to interact with cavin 2 (Bastiani *et al*., 2009; Briand *et al*., 2010; Hansen and Nichols, 2010; Liu *et al*., 2008; Nabi, 2009). Cavin 4 distribution is perturbed in human muscle disease associated with caveolin-3 dysfunction, identifying cavin 4 as a novel muscle

disease candidate caveolar protein (Bastiani *et al*., 2009). Over expression of this protein in the heart is sufficient to induce cardiac contractile dysfunction (Hansen and Nichols, 2010). In contrast with cavin 2 and cavin 3, cavin 4 expression levels are not affected by the absence of cavin 1 (Bastiani *et al*., 2009).

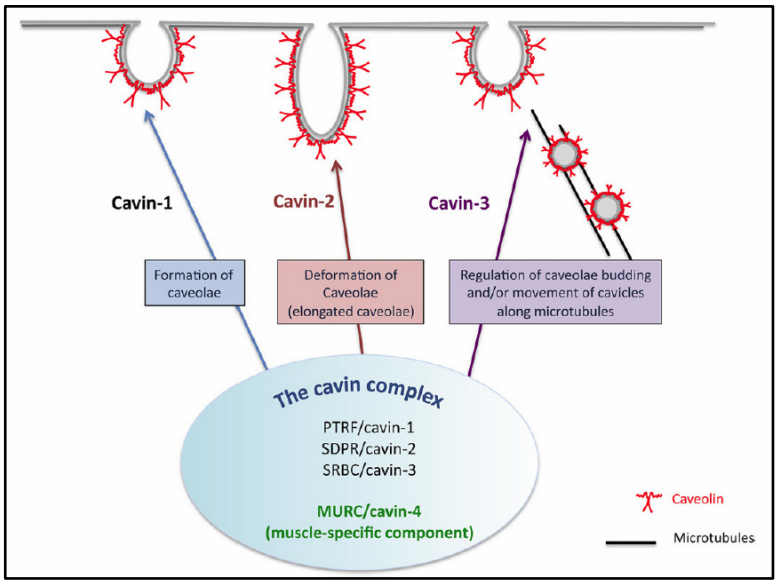

Figure 1.4. Regulation of caveolae morphology and dynamics by cavin family members. Recent data revealed the existence a multimeric protein complex containing all cavin members, which associate with caveolins at the plasma membrane. Individual overexpression or downregulation of each cavin member has an effect on biogenesis, morphology or dynamics of the caveolae structures. Cavin 1 is recruited by caveolins to plasma membrane caveolar domains and is required for caveolae formation. Cavin 2 alone does not increase caveolae number but induces changes in caveolae morphology, which turns to appear distended. Cavin 3 still associates with caveolin upon caveolae budding to form vesicles and its absence markedly impairs intracellular caveolin-1 traffic along microtubules. Cavin 4, which has an expression restricted to cardiac and muscle tissues (parallel that of caveolin-3), constitutes the muscle-specific component of the cavin complex and associates with muscle-caveolae. (Adapted from Briand, 2010).

1.5 Objectives

It has recently been shown that cavins are essential caveolar components and that cavins and caveolins, other major caveolar proteins, are interdependent (Hill *et al*., 2008, Vinten *et al*., 2005). *In vivo* studies revealed that cavin 1 knockout (KO) mice lack caveolae, are insulin resistant and present a lipodystrophic phenotype (Liu *et al*., 2008) and indeed, recently published data identified cavin 1 as a locus for human lipodystrophy (Garg, 2011; Hayashi *et al*., 2009). Studies in cavin 2 KD cells have also revealed that cavin 2 is essential for cavin 1 recruitment to the caveolae and that cavin 2 acts as the caveolae membrane curvature-inducing component (Hansen *et al*., 2009).

Considering the importance of caveolae in the proper functioning of adipocytes and knowing that cavin 1 and cavin 2 are essential caveolar proteins we decided to study the role of cavin 1 and cavin 2 in adipocyte function. To do so, we obtained 3T3-L1 cell lines with a reduced expression of cavin 1 or cavin 2 by a small interfering RNA (siRNA) strategy. We analyzed the differentiation capability, caveolae morphology, insulin-mediated glucose uptake and insulin signaling cascade in these KD cell lines.

2. Materials and Methods

2.1 Entities

This work was carried out at the Department of Biochemistry and Molecular Biology, Faculty of Biology, University of Barcelona (FB/UB) and at the Institute for Research in Biomedicine, Parc Científic of Barcelona (IRB,Barcelona/PCB).

2.2 Materials

Table 2.1 - List of reagents and materials used in this work and respective references.

Products	References
2-deoxy[H3]-glucose	American Radiolabeled, cat#ART-103A
2-deoxyglucose	Sigma, cat#D8375
D-(+)-glucose	Sigma, cat#G8270
Acrylamide solution (30%)	National Diagnostics,cat#EC-890
Aprotinin	Sigma, cat#A6279
APS	BioRad,cat#161-0700
Broad range molecular weight (pre-stained)	BioRad cat#161-0318
Bromophenol blue	BioRad,cat#161-0404
BSA- Fatty acid free	Sigma, cat#A6003
CS	BioWhittaker 14-401F
Dexamethasone-water soluble	Sigma, cat#D2915
DMEM	Gibco,cat#41966-052
DMSO	Sigma, cat#D2650
EDTA	Calbiochem, cat#324503
FBS	Gibco, cat#10270-106
Glycine	Roche, cat#03117251001
Glycerol	Sigma, cat#G5516
HEPES	Sigma, cat#H3375
Hydrogen Peroxide	Sigma, cat#H1009
IBMX	Sigma, cat#I-7018
Insulin Human	Lilly, cat#KG5-WEF-179
Igepal CA630	Sigma, cat#I8896
Isopropanol	Panreac, cat#141090
Leupeptin	Sigma, cat#L2884
Luminol	Fluka, cat#09253
Methanol	Panreac, cat#141091
Mini-Protean® System III	Biorad
Mini-Protean® TransBlot Cell System	Biorad
Oil Red O	Sigma, cat#O-0625
p-Coumaric acid	Fluka, cat#2820
Paraformaldehyde	Fluka, cat#76240
Penicillin-Streptomycin	Gibco,cat#15140-163
Pepstatin	Sigma, cat#A5318
Radiographic films	Fujifilm, cat#4741008389
Pierce® BCA Protein Assay Reagent	Thermo Scientific, cat#23225
PMSF	Merck, cat#1,07349,0005
Poly-L-Lysine	Sigma, cat#P1524
PEI	Polysciences Inc., cat#23966
ProLong® Gold antifade reagent	Invitrogen, cat#P36930
Protein G-sepharose beads	Sigma, cat#P3296

Puromycin dihydrochloride solution	Sigma, cat#P9620
PVDF Membrane	ImmobilonTM-P; Millipore, #IPVH00010
Rosiglitazone	SmithKline Beecham
Scintillation liquid	Ecolite, cat#882475
SDS	Panreac, cat# 142363
Sodium deoxycholate	Sigma, cat#D6750-25G
Sodium pyruvate	Sigma, cat#P2256
Sucrose	Sigma, cat#S9378
TEMED	Biorad,cat#161-0801
Triglycerides assay kit	BioSystems, cat#11528
Triton-X-100	Merck, cat#8603
Tris-base	Panreac, cat#141940
Tween-20	Sigma, cat#P1379
Trypsin	Invitrogen, cat#25300-062
Ultracentrifuge tubes	Beckman Coulter, cat#358126

2.2.1 Antibodies

Table 2.2 - Primary antibodies used in this work for Western blot (WB), Immunoprecipitation (IP) and Immunolocalization(IL).

Target	Supplier	Raised in	MW (kDa)	Used for		
				WB	IP	IL
β-actin	Sigma cat# AC-15	Mouse	45	1:10000		
Cavin-1	Suplied by Dr.Paul Pilch	Rabbit	60	1:1000		1:200
Cavin-2	Suplied by Dr.Paul Pilch	Rabbit	68	1:1000		1:200
Caveolin-1	Transduction laboratories	Rabbit	22	1:1000		1:200
GLUT4	Generated in our laboratory	Rabbit	55	1:1000		1:200
Perilipin	Upstate Biotech, Cat#AB10200	Rabbit	64	1:1000		1:200
Akt	Cell signaling, Cat#9272	Rabbit	60	1:1000		
InsR β-chain (4B8)	Cell signaling, Cat#3025	Rabbit	95	1:500		
PI3K (p85 subunit)	Upstate Biotech, Cat#06-195	Rabbit	85	1:1000		
IRS-1	Cell signaling, Cat#2382	Rabbit	180	1:500	3µL/500µg	
Phospho-Tyr residues	Upstate Biotech, Cat#05-321	Mouse	-	1:1000	3µL/500µg	
Phospho-Akt (Ser473)	Cell signaling, Cat#9271	Rabbit	60	1:1000		
ATGL	Cell signaling, Cat#2138	Rabbit	54	1:1000		
FABP4	Cell signaling, Cat#2120S	Rabbit	15	1:1000		

Table 2.3 - Secondary antibodies used in this work for Western blot (WB), Immunofluorescence (IF) and Freeze Drying (FD).

Antibody description	Supplier	Used for		
		WB	IF	FD
Goat Anti-Rabbit IgG (H+L)	Jackson Immuno Research 711-035-152	1:10000		
Donkey Anti-Mouse IgG (H+L)	Jackson Immuno Research 715-035-150	1:10000		
Donkey Anti-Rabbit IgG (H+L)	Jackson Immuno Research 711-165-152		1:200	
Goat Anti-Rabbit IgG (H+L)	Jackson Immuno Research 111-205-144			1:30

Depending on the technique, we used antibodies commercially conjugated with horseradish peroxidase (Western blot), fluorochromes (Immunofluorescence) and colloidal gold particles (Freeze-drying).

Primary and secondary antibodies used in Western blot were prepared in 5% (w/v) non-fat dry milk in PBS1x excepting PI3K (p85 subunit) and phospho-tryrosine residues antibodies. These were prepared in 5% (w/v) BSA in PBS1x.

Antibodies used in immunolocalization were prepared in 10% (v/v) FBS in PBS1x and were centrifuged at 16000rcf, 4ºC for 5 minutes, before being used.

2.2.2 Cell Lines

2.2.2.1 3T3-L1

The main cell line used during this thesis was the *Mus musculus* (mouse) embryo 3T3-L1 cell line acquired from ATCC (ATCC CL-173™). L1 is a continuous substrain of 3T3 (*Swiss albino*) developed through clonal isolation. The cells undergo a pre-adipose to adipose like conversion as they progress from a rapidly dividing to a confluent and contact inhibited state. Cells were manipulated as stipulated by ATCC.

2.2.2.2 Hek293T

This is the 293 clone of transformed human embrionary kidney cell lines, generated by infection with the adenovirus 5 (Ad 5) DNA. This cell line contains the "early expression region 1" (E1) from Ad 5, thus allowing the growth of adenoviruses lacking E1. 293 cells are efficiently infected by adenoviruses and are generally used for adenovirus amplification and their quantification. Hek 293T cells are a subline of Hek 293 cells which stably express SV40 large T antigen allowing episomal replication of plasmids containing an origin of replication of SV40.

2.3 Methods

2.3.1 Cell Culture

Table 2.4 - Composition of culture mediums used in cell culture protocols

10% CS medium	
Reagent	***Final Concentration***
DMEM	4,5g/L Glucose; 2mM L-Glutamine;0,11 g/L Pyruvate
Penicillin-Streptomycin	100U/mL-100µg/mL
HEPES	25mM, pH=7.4
CS	10% (v/v)
Puromycin dihydrochloride	3µL/mL
10% FBS medium	
Reagent	***Final Concentration***
DMEM	4,5g/L Glucose; 2mM L-Glutamine;0,11 g/L Pyruvate
Penicillin-Streptomycin	100U/mL-100µg/mL
HEPES	25mM, pH=7.4
FBS	10% (v/v)
Puromycin dihydrochloride	3µL/mL
Fasting Medium	
Reagent	***Final Concentration***
DMEM	4,5g/L Glucose; 2mM L-Glutamine;0,11 g/L Pyruvate
Penicillin-Streptomycin	100U/mL-100µg/mL
HEPES	25mM, pH=7.4
BSA	0,2% (w/v)
Freezing Medium	
Reagent	***Final Concentration***
FBS	90% (v/v)
DMSO	10%(v/v)
Differentiation Medium 1	
Reagent	***Final Concentration***
DMEM	4,5g/L Glucose; 2mM L-Glutamine;0,11 g/L Pyruvate
Penicillin-Streptomycin	100U/mL-100µg/mL
HEPES	25mM, pH=7.4
FBS	10% (v/v)
Insulin	5µg/mL
Dexamethasone	0,25µM
IBMX	0,5mM
Rosiglitazone	1µM
Puromycin dihydrochloride	3µL/mL
Differentiation Medium 2	
Reagent	***Final Concentration***
DMEM	4,5g/L Glucose; 2mM L-Glutamine;0,11 g/L Pyruvate
Penicillin-Streptomycin	100U/mL-100µg/mL
HEPES	25mM, pH=7.4
FBS	10% (v/v)
Insulin	5µg/mL
Puromycin dihydrochloride	3µL/mL
Hek293T Medium	
DMEM	4,5g/L Glucose; 2mM L-Glutamine;0,11 g/L Pyruvate
Penicillin-Streptomycin	100U/mL-100µg/mL
FBS	10% (v/v)
HEPES	25mM, pH=7.4

2.3.1.1 Defrosting Cells (3T3-L1 Cell Lines)

Cryotubes containing fibroblasts were taken from the liquid nitrogen storage tank and submerged in a bath warmed at 37ºC. As soon as the solution started to defrost cells were transferred to a 25cm^2 culture flask with 10%CS medium (table 2.4). Cells were incubated at 37ºC, 95% humidity and 10% CO_2. After 12 hours the medium was renewed.

2.3.1.2 Growing/Differentiating cells (3T3-L1 Cell Lines)

Fibroblasts were maintained in 75 cm^2 culture flasks in 10%CS medium (table 2.4) and incubated at 37ºC, 95% humidity and 10% CO_2. Before reaching confluence, cells were washed twice with sterile PBS1x (137mM NaCl; 2,7mM KCl; 4,3mM Na_2HPO_4; pH=7,4) and trypsinized until cells were fully detached. Cells were then counted in a Neubauer chamber and 240.000 cells were seeded per 10cm ø plate. Two days after reaching confluence, about 9 days after seeding, cells were induced to differentiate by changing to differentiation medium 1 (table 2.4). After 48 hours medium was changed to differentiation medium 2 (table 2.4). Two days later, medium was changed to 10% FBS medium (table 2.4). Adipocytes were maintained in 10% FBS medium and every two days the medium was renovated.

2.3.1.3 Freezing cells (3T3-L1 Cell Lines)

Fibroblast still in the exponential growth phase were washed twice with sterile PBS1x and trypsinized. Cells were recovered to falcon tubes and spun down at 2000 rpm for 3 minutes. The supernatant was discarded and cells were resuspended in ice cold freezing medium (table 2.4). Cells were transferred to cryovials and stored at -80ºC inside a cryocooler. After 24 hours vials were moved to liquid nitrogen storage tank.

Cell culture protocols used for Hek293T cell line were similar to those described above. However, cells were maintained in Hek293T medium and were not induced to differentiate.

2.3.2 Lentiviral Production and Adipocyte Infection

For the lentiviral production, we used siRNA obtained from the Functional Genomics Core Facility-Institute for Research in Biomedicine Barcelona library. The library contained five different siRNAs for cavin 1 and four for cavin 2, in both cases the siRNAs were cloned in pLKO.1 plasmid.

Table 2.5 – Nucleotide sequences of siRNAs used for cavin1 and cavin 2 knockdowns.

siRNA	Oligo Sequence
Cavin1.1	5'-CCGGGCAGAGTGTTTGGTGGATAAACTCGAGTTTATCCACCAAACACTCTGCTTTTTG-3'
Cavin1.2	5'-CCGGGATAAAGAAACTGGAGGTCAACTCGAGTTGACCTCCAGTTTCTTTATCTTTTTG-3'
Cavin1.3	5'-CCGGGCCTTTCACCTTCCACGTCAACTCGAGTTGACGTGGAAGGTGAAAGGCTTTTTG-3'
Cavin1.4	5'-CCGGGCGCTCCAAGACCGCTGTCTACTCGAGTAGACAGCGGTCTTGGAGCGCTTTTTG-3'
Cavin1.5	5'-CCGGAGCGTCAGCAAGTCGCTGAAACTCGAGTTTCAGCGACTTGCTGACGCTTTTTTG-3'
Cavin2.1	5'-CCGGCCTGGATAAATTGGTCAACATCTCGAGATGTTGACCAATTTATCCAGGTTTTTG-3'
Cavin2.2	5'-CCGGCCTCTCCTTTGGTCGTAAGAACTCGAGTTCTTACGACCAAAGGAGAGGTTTTTG-3'
Cavin2.3	5'-CCGGCCAGCCTCAAGAAAGTCGATACTCGAGTATCGACTTTCTTGAGGCTGGTTTTTG-3'
Cavin2.4	5'-CCGGGAGAACCAGCACAACATGGAACTCGAGTTCCATGTTGTGCTGGTTCTCTTTTTG-3'

2.3.2.1 Tranfection of Hek293T cells

Viral production was performed in Hek293T cells. Cells were transfected using the PEI method. Plasmid pCMVDR7.8 was used as packaging plasmid and pMD2G as envelope plasmid.

Hek293T cells were seeded in 10cm ø plates so that they were confluent in the next day. Plates contained 10mL of Hek293T medium (Without HEPES) (table 2.4) and incubation conditions were the same as those used for adipocytes (37ºC, 95% humidity and 10% CO_2). Then 10µg of siRNA, 7µg of pCMVDR7.8 and 3µg of pMD2G were mixed and taken to a final volume of 1560µL with sterile 150mM NaCl. 78µL of PEI (from 1mg/mL, pH=7.0) were then added and the mix was vortexed for 20 seconds. After 15 minutes, the mix was added to the plate and 7-8 hours later the medium was removed and cells were incubated with 5mL of Hek293T medium. Incubation temperature was changed to 33ºC.

2.3.2.2 Virus recovery and purification

Approximately 24 hours after transfection culture medium was recovered, centrifuged at 2500 rpm for 10 minutes at 4ºC, then filtered through 0,45µm filter and stored at 4ºC. Cells were incubated with another 5 mL of Hek293T medium and again, 24 hours later the medium was recovered, centrifuged and filtered as described above.

Viruses were then purified through ultracentrifugation on a sucrose cushions. To do so the recovered medium was placed in ultracentrifuge tubes and using a syringe, 4ml of 20% sterile sucrose was carefully added to the bottom of the tube. Medium were centrifuged at 26000rpm for 1h30 minutes at 4ºC. The medium and sucrose were discarded, tubes were dried and the pellet containing viruses was resuspended in 100µl of DMEM with 100U/mL-100µg/mL penicillin-streptomycin.

2.3.2.3 Infection of 3T3-L1 fibroblasts

Adipocyte infection was performed in 6-well plates and 20.000 3T3-L1 fibroblasts (low passage) were seeded per well. Fibroblasts were cultured in 10% CS medium (table 2.4) without puromycin and incubated at 37ºC, 95% humidity and 10% CO_2. Four to five hours after seeding, the viruses produced and purified as described in the last section were added to the medium and the incubation temperature was changed to 33ºC. Approximately 12 hours later the medium was renovated and the temperature was returned to 37ºC. Two days later the medium was changed to complete 10% CS medium (table 2.4) to select infected cells.

2.3.3 Obtention of whole cell lysates

Plates of 10cm ø with cultured cells were washed twice with PBS1x (137mM NaCl; 2,7mM KCl; 4,3mM Na_2HPO_4; pH=7,4) and incubated for 30 minutes on ice with 1mL of RIPA buffer (50mM Tris-base, pH=7,4; 150mM NaCl; 1% (v/v) Igepal CA630; 0,5% (w/v) Sodium deoxycholate; 0,1% (v/v) SDS) containing a protease inhibitor cocktail (1µg/mL Pepstatin; 1µg/mL Leupeptin; 0,5mM PMSF; 10µg/mL Aprotinin). Cells were then scrapped off the plates, transferred to eppendorfs and homogenized using a syringe with a 25G needle. After homogenization, lysates were placed on a shaker for 30 minutes at 4ºC and spun down for 10 minutes at 16000rcf at 4ºC. Supernatant was recovered and protein concentration was determined as described in the section below. Lysates were stored at -80ºC.

2.3.4 Protein Quantification (BCA method)

In this thesis protein quantification was performed using the Pierce® BCA Protein Assay Reagent which does not interfere with the detergents used in the lysis buffers.

A standard curve from 0 to 20µg was generated loading the appropriate volumes of 1mg/mL BSA (included in the kit) into an ELISA plate and 5µL of protein lysate were used in the quantification (all volumes done in duplicates). A reactive solution was prepared according to the manufacturer's instructions (mix solution A with B in a 50:1 ration) and 200µL were loaded in each

well. Plates were incubated at 37ºC for 15 minutes and absorbance was read at 562nm in an ELISA plate reader, Biowhittaker Microplate Reader 2001.

2.3.5 Protein detection by SDS-PAGE electrophoresis and Western blot

Table 2.6 – Stacking gel (3.3%) and Running gel (7.5%, 10%) chemical composition.

Stacking gel (5mL/gel)			**Running gel (10mL/gel)**			
	3,3%	**Final Con.**		**7,5%**	**10%**	**Final Con.**
Acrylamide 30%	0,65mL	3,3%	Acrylamide 30%	2,5mL	3,2mL	7,5%/10%
Tris-HCl 0,5M, pH=6,8	1,25mL	0,125M	Tris-HCl 1,5M, pH=8,8	2,5mL	2,5mL	0,375M
SDS 10%	50µL	0,1%	SDS 10%	100µL	100µL	0,1%
APS 10%	50µL	0,1%	APS 10%	100µL	100µL	0,1%
TEMED	7µL	6,6mM	TEMED	10µL	10µL	2,2mM
H_2O Milli-Q	Up to 5mL		H_2O Milli-Q	Up to 10mL		

Samples were prepared with the desired amount of protein lysates and LSB4x (250mM Tris-HCL, pH=6,8; 40% (v/v) glycerol; 8% (w/v) SDS; 0,02% (w/v) bromophenol blue) was added, diluting it four times, then samples were boiled at 95ºC for 5 minutes.

Depending on the molecular weight of the protein of interest, the stacking and running gels were prepared according to table 2.6 and samples were loaded into the stacking gel. The electrophoresis was performed at RT and ran at 100V throughout the time for a good protein separation (which depends on the protein of interest and gel percentage), using electrophoresis buffer 1x (25mM Tris-base; 190mM glycine; 0,1% (v/v) SDS). In the development of this thesis we used Mini-Protean® III Electrophoresis System.

After the protein separation, proteins were transferred to a 0,2µm PVDF membrane. For this end we used the Mini-Protean® TransBlot Cell System. The protein transfer procedure occurred on ice at 250mA for 120 minutes using transference buffer 1x (25mM Tris-base, pH=8,3; 192mM glycine; 20% (v/v) Methanol).

Once the transference was completed, membranes were incubated with the blocking solution (10% (w/v) non-fat milk in 0,5% (v/v) Tween-20-PBS1x), for 1hour at RT in a rocking platform (if PI3K-p85 subunit or phospho-tryrosine residues antibodies were to be used, the blocking solution was 5% (w/v) BSA in PBS1x). Membranes were then incubated with primary antibody (table 2.2), o/n at 4ºC. After incubation with primary antibody the membranes were washed with washing solution (0,01%(v/v) Triton-X-100-PBS1x) at RT in a rocking platform, for 30 minutes, changing the solution every 10 minutes. Membranes were then incubated with secondary antibody (table 2.3), for 2 hours at 4ºC, and washed again as described above.

For the chemioluminescent antibody detection, membranes were incubated for 1 minute with a mixture (1:1) of ECL solution 1 (0,1M Tris-HCL, pH=8,5; 2,5mM luminol; 0,39mM p-Coumaric acid) and ECL solution 2 (0,1M Tris-HCL, pH=8,5; 5,6mM hydrogen peroxide) and then the membrane was exposed to a x-ray film. The exposition times varied depending on the intensity of the signal. Films were revealed in a FPM100A, Fujifilm® equipment.

2.3.6 Immunoprecipitaton

Immunoprecipitation was performed in differentiated adipocytes grown in 10 cm ø plates. First cells were serum-fasted, washing twice with PBS1x (137mM NaCl; 2,7mM KCl; 4,3mM Na_2HPO_4; pH=7,4) and incubating them with fasting medium (table 2.4) for 3 hours at 37ºC, 95% humidity and 10% CO_2.

After fasting, cells were incubated with 0nM or 100nM insulin for 30 minutes at 37ºC and then lysed as described in section 2.3.3 but using lysis buffer (50mM HEPES; 10mM EDTA; 150mM NaCl; 1% (v/v) Igepal CA630; pH=7,4) with protease (1µg/mL Pepstatin; 1µg/mL Leupeptin; 0,5mM PMSF; 10µg/mL Aprotinin) and phosphatase (10mM $Na_4P_2O_7$; 100mM NaF; 1mM Na_3VO_4) cocktail inhibitors instead of RIPA buffer.

Protein concentration of the lysates was determined, as described in section 2.3.4, and samples with 500 µg of protein were prepared. 30µl of protein G-sepharose beads and 3µl of specific antibody were added to each sample and they were incubated o/n at 4ºC in an orbital agitator.

In the next day samples were centrifuged at 3000rpm for 3 minutes at 4ºC and the supernatant was recovered and stored at -80ºC. Pellet was washed three times with buffer A (50mM HEPES; 10mM EDTA; 150mM NaCl; pH=7,4) with phosphatase cocktail inhibitor (10mM $Na_4P_2O_7$; 100mM NaF; 1mM Na_3VO_4). Washings were performed adding buffer A and centrifuging samples at 3000rpm for 3 minutes at 4ºC and discarding the supernatant. After the washings LSB4x (250mM Tris-HCL, pH=6,8; 40% (v/v) glycerol; 8% (w/v) SDS; 0,02% (w/v) bromophenol blue) containing 0,1M DTT was added to each sample and samples were boiled at 95ºC for 5 minutes. Results were analyzed by western blot.

2.3.7 Glucose Transport

Differentiated adipocytes grown in 6-well plates were serum-fasted, washing twice with PBS1x (137mM NaCl; 2,7mM KCl; 4,3mM Na_2HPO_4; pH=7,4) and incubating with 10mL of fasting medium (table 2.4) for 3 hours at 37ºC, 95% humidity and 10% CO_2.

After fasting, cells were washed three times with PBS1x and 0,9mL of Krebs-Ringer-HEPES buffer (137mM NaCl; 4,7mM KCl; 1,18mM $MgSO_4.7H_2O$; 1,18mM KH_2PO_4; 2,5mM $CaCl_2.H_2O$; 20mM HEPES, pH=7.4; 0,2% (w/v) BSA; 2mM Sodium pyruvate; pH=7,4) were added to each well.

Cells were then incubated, at 37ºC for 30 minutes, with different concentrations of insulin (0nM, 1nM, 10nM, 100nM).

After insulin action, 100µL of substract solution (Krebs-Ringer-HEPES buffer; 100µM 2-deoxyglucose; 1µCi/ml 2-deoxy[H3]-glucose) were added to each well and 5 minutes later the transport was stopped adding STOP Buffer at 4ºC (50mM D-(+)-glucose in PBS1x). To eliminate the non-incorporated radioactivity, cells were washed three times with STOP buffer at 4ºC. Once the wells were dried, 800µL of lysis buffer (100mM NaOH; 0,1% (v/v) SDS) was added and cells were scrapped off and homogenized with the pipette.

To evaluate the amount of incorporated radioactivity, 250µL of lysate were mixed with 3mL of scintillation liquid and radioactivity was measured in a β-counter, Tri-CARB 2100TR, Packard®. Protein content in the lysate was determined using the Pierce® BCA Protein Assay Reagent as described above in section 2.3.4 but loading 10µL of lysate instead of 5µL.

2.3.8 Immunolocalization

Immunolocalization was performed in permeabilized whole-cell or in plasma membranes of differentiated adipocytes grown in glass coverslips (12 mm diameter). In some cases a previous stimulation with insulin was performed.

2.3.8.1 Insulin stimulation

For the insulin stimulation, first cells were serum-fasted, as described in section 2.3.6. Then cells were incubated with or without 100 nM insulin for 30 minutes at 37ºC. After insulin action, cells were washed three times with PBS1x (137mM NaCl; 2,7mM KCl; 4,3mM Na_2HPO_4; pH=7,4).

2.3.8.2 Plasma membrane Lawns

If immunolocalization was to be done in plasma membrane lawns, the following protocol was performed.

Cells grown in glass coverslips were washed twice with PBS1x and then incubated with poly-L-lysine (0,5mg/mL) in PBS1x for 1 minute at RT. The solution was removed and cells were washed again with PBS1x. Cells were then swollen by incubation with KHMgE 1/3x buffer (1x concentration, 70mM KCl; 30mM HEPES, 5mM $MgCl_2$; 3mM EGTA; pH=7,5) for 5 minutes at RT. The medium was removed and cells were placed in KHMgE 1x buffer and then ruptured using a plastic Pasteur pipette. Membranes were washed with PBS1x.

2.3.8.3 Immunolocalization

Plasma membrane lawns or whole adipocytes, grown in glass coverslips, were fixed in 3% (v/v) PFA in PBS1x for 15 minutes at RT. PFA was removed and cells/membranes were washed three times with PBS1x and then incubated, for 10 minutes at RT, with 50mM NH_4Cl in PBS1x. NH_4Cl solution was removed and cells/membranes were placed in 20mM glycine in PBS1x for another 10 minutes at RT. If the protocol was being done in whole-cells, a permeabilization step was necessary and so, glycine was removed and cells were incubated with 0,1% (v/v) Triton X-100 in PBS1x, for 10 minutes at RT. Then cells/membranes were washed three times with PBS1x and nonspecific binding sites were blocked with 10% (v/v) FBS in PBS1x, for 30 minutes at RT.

Incubation with primary antibodies (table 2.2) was done for 1 hour at RT, placing a 25µL drop of antibody solution in each coverslip. After the incubation cells/membranes were washed three times with PBS1x and then incubated with the secondary antibody (table 2.3), as described for the primary. During the incubation, cells/membranes were protected from light since the fluorochrome attached to the secondary antibody is photosensitive. Cells/membranes were washed again three times with PBS1x and dried at RT.

Coverslips were mounted with ProLong® Gold antifade reagent and viewed in a Leica TCS SPE spectral confocal microscope.

2.3.9 Freeze-Drying

2.3.9.1 Obtention of plasma membrane lawns and immunogold

Differentiated adipocytes, grown in glass coverslips, were disrupted as described in section 2.3.8.2 in order to obtain plasma membrane lawns and all the procedure was performed on ice cold plates. Then membranes were fixed with 3% (v/v) PFA in PBS1x (137mM NaCl; 2,7mM KCl; 4,3mM Na_2HPO_4; pH=7,4) for 15 minutes. PFA was removed and membranes were washed three times with PBS1x. Antibody nonspecific binding sites were blocked with 10% (v/v) FBS in PBS1x, for 30 minutes. After blocking, the incubation with primary antibody (table 2.2) was done for 1 hour, placing a 25µL drop of antibody solution in each coverslip. After the incubation, membranes were washed three times with PBS1x and then incubated with the secondary antibody (table 2.3), as described for the primary. Membranes were washed again three times with PBS1x.

2.3.9.2 Freeze-Drying

Membranes were fixed with 2,5% glutaraldehyde in PBS1x for 15 minutes and then washed with H_2O Milli-Q and cryoprotected with 10% methanol. The sample was ultrarapidly frozen impacting it onto a block of cooled copper (slam-freezing) and then transferred to a freeze-drying device (BAF-

060, Bal-Tec, Liechnstein) and the surface ice was removed at -90ºC, 10^{-7}mbar for 90 minutes. A thin layer of platinium (23º, 1nm) was evaporated rotationally onto the sample to produce replicas of the surface of the membrane and next replicas were reinforced with a carbon layer (75º, 10nm). Replicas were separated from the coverslip with 30% hydrofluoric acid and the organic material was digested with bleach for 12 hours. Finally replicas were washed with H_2O Milli-Q, mounted on copper grids and covered with Formvar resin. Observations were done in a JEOL 1010 Transmission Electron Microscope.

2.3.10 Oil red staining

Oil Red staining is a technique used to stain neutral lipid inside the cell. For this protocol a 8,5mM OilRed O stock solution was prepared diluting Oil Red O in isopropanol and letting it stirring overnight, at RT. The stock solution was then filtered with 0,2µm filter.

Differentiated adipocytes were fixed with 3% PFA for 15 minutes at RT. The PFA was removed and cells were washed with 60% isopropanol. The cells were then incubated with working solution (60% OilRed O stock; 40% H_2O Milli-Q), previously filtered with 0,2µm filter, for 10 minutes at RT. Working solution was removed and cells were washed three times with H_2O Milli-Q. Adipocytes were observed in a phase contrast microscope.

2.3.11 Triglyceride Quantification

Triglyceride quantification in total lysates was performed using the Biosystems Triglyceride assy kit. Differentiated adipocytes were lysed as described in section 2.3.3 but using an homogenization buffer (0,25M Sucrose; 2mM EGTA; 20mM HEPES; pH=7,4) with protease inhibitors (1µg/mL Pepstatin; 1µg/mL Leupeptin; 0,5mM PMSF; 10µg/mL Aprotinin) instead of RIPA buffer.

A standard curve from 0 to 200mg/dL was generated loading serial dilutions of the 200mg/dL triglycerides standard solution (included in the kit) into the ELISA plate and 10µL of the lysate were used in the quantification (done in duplicates). Then 200µL of reactive solution (included in the kit) were added to each well and plates were incubated 5 minutes at 37ºC. After incubation plates were read at 500nm.

3. Results

3.1 Obtention of 3T3-L1 cell lines deficient in Cavin 1 and Cavin 2

In the development of this thesis we wanted to study the role of cavin 1 and cavin 2 in the functioning of adipocytes. The first step to achieve our goal consisted in developing one 3T3-L1 multiclonal cell line deficient in cavin 1 and another one in cavin 2.

To reduce the expression of these proteins we used a post-transcriptional gene silencing approach. The KD consisted in infecting 3T3-L1 pre-adipocytes (fibroblasts) with lentiviruses able to integrate in the genome of these cells and express hairpin siRNA sequences. As decribed in section 2.3.2 we had five siRNA sequences for cavin 1 and four sequences for cavin 2.

We were not able to grow cells infected with lentivirus containing the sequences cavin1.3 and cavin1.4, so we managed to obtain four cell lines for cavin 2 KD, three for cavin 1 KD and a control cell line in which we used a scrambled siRNA sequence. Reduction in cavin expression levels was assessed by western blot assay using lysates of both fibroblasts and differentiated adipocytes (figure 3.1). As represented in figure 3.1, in adipocytes we could obtain a reduction of cavin 1 in all cavin1.1, cavin1.2 and cavin1.5 cell lines. For cavin 2, we obtained a greater reduction on clones cavin2.3 and cavin2.4. In fibroblasts we only detected cavins in control cells although at low levels.

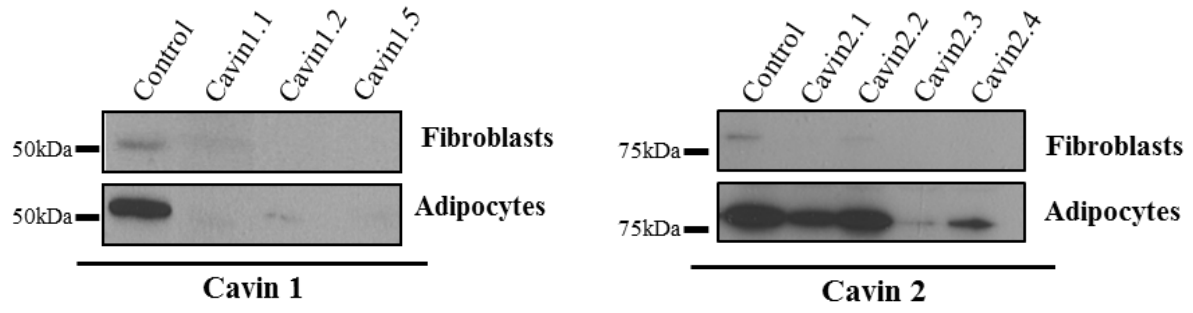

Figure 3.1 – Cavin 1 and cavin 2 expression in 3T3-L1 fibroblasts and adipocytes infected with lentiviruses containing scrambled or different cavin siRNA sequences of both proteins. 50µg of protein from cell lysates were used to analyze cavin 1 and cavin 2 expression by SDS-PAGE followed by western blot assay with an anti-cavin1 and cavin 2 specific antibodies.

Taking into account the level of protein reduction, the KD stability through the cell passages and the differentiation capability, we selected one KD clone for each cavin. The two selected clones were cavin1.5 and cavin2.3 for cavin 1 and cavin 2 KDs, respectively. In figure 3.2 it is represented the cavin 1 and cavin 2 reduction obtained in both selected clones. For cavin1.5 clone we were able to obtain a reduction of 65% in the expression of cavin 1. Regarding cavin2.3 clone we obtained a KD of 97% in cavin 2 expression. We also observed that cavin1.5 cells, besides the reduction in cavin 1

expression, also had lower levels of cavin 2 (48% less than control cells). The same observation was made for cavin2.3, besides the lower levels of cavin 2, these cells had a reduction of 54% in the expression of cavin 1.

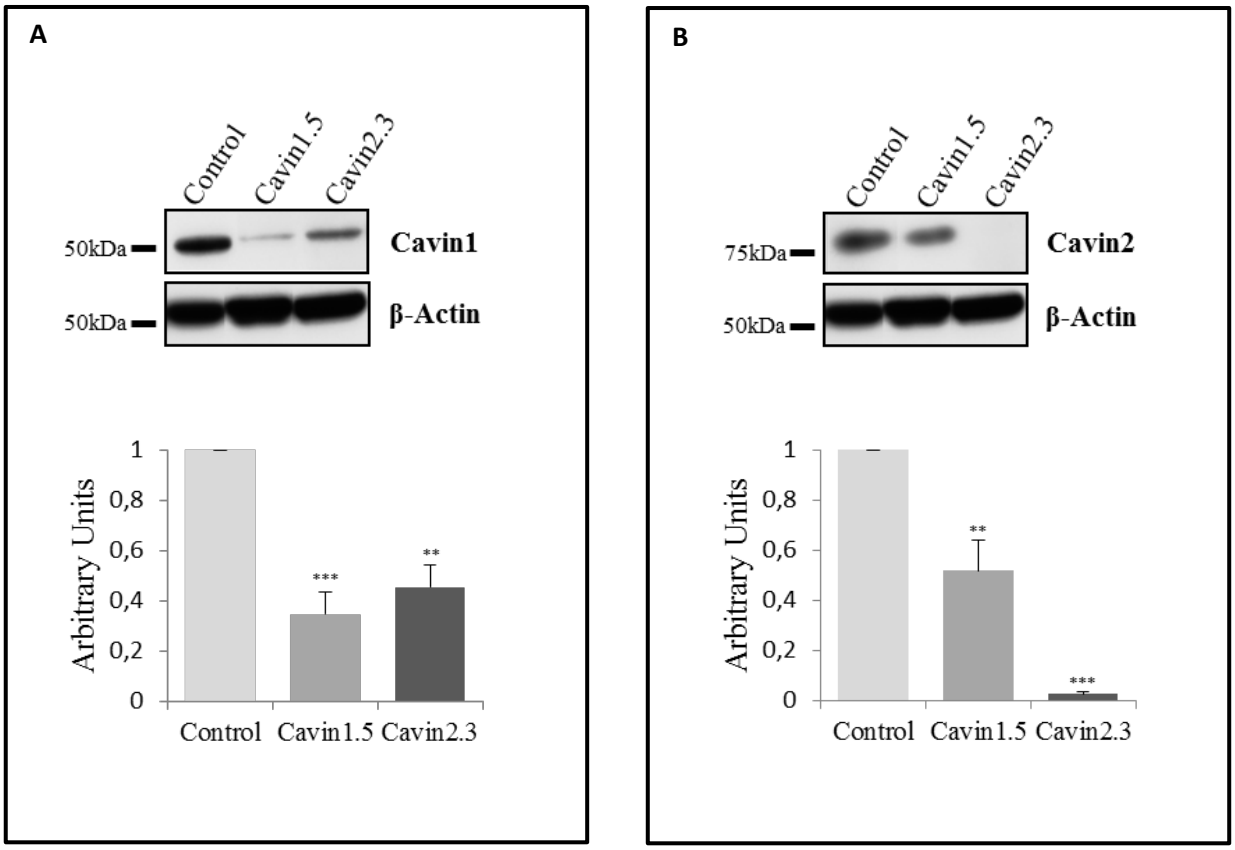

Figure 3.2 – siRNA mediated downregulation of cavin 1 (A) and cavin 2 (B) expression in 3T3-L1 adipocytes. 50µg of protein from cell lysates were used to analyze cavin 1 and cavin 2 expression by SDS-PAGE followed by western blot with anti-cavin 1 and cavin 2 antibodies. Cell lysates were recovered 12 days after the induction of differentiation. In the western blot band quantification, each data point represents the mean ±SEM derived from six independent experiments normalized to control cells. One-way ANOVA test was performed between KD and control cells. ***, P≤0,001;**, P≤0,01.

In order to confirm the reduction in cavin 2 levels and to observe its membrane distribution, in both cavin1.5 and cavin2.3 cells, we performed an immunolocalization of cavin 2 in plasma membrane lawns of these cells.

Analysing both figure 3.3 and figure 3.4 we observe that cavin 2 levels are reduced in both KD cells when compared with control cells which is accordant with the western blot results and because cavin 2 is localized in caveolae we can also observe that caveolae are absent/altered in KD cells (figure 3.4 and 3.5). These results indicate that cavin 2 is important for caveolae correct formation. The absent/altered caveolae are even more evident in figure 3.5. Cavin2.3 KD cells have

less caveolae and some of them show a torus shape (green arrows) and others appear completely flat (white arrows).

The level of reduction in the cavin 2 levels could not be quantified using the images in figure 3.3 since they were acquired using different settings, otherwise no signal would be observed in cavin2.3 KD cells images. These changes were done so that one could observe the differences in caveolae structure.

The same experiments were performed using anti-cavin 1 antibody but the antibody our laboratory possessed failed to work properly in immunoflourescence experiments.

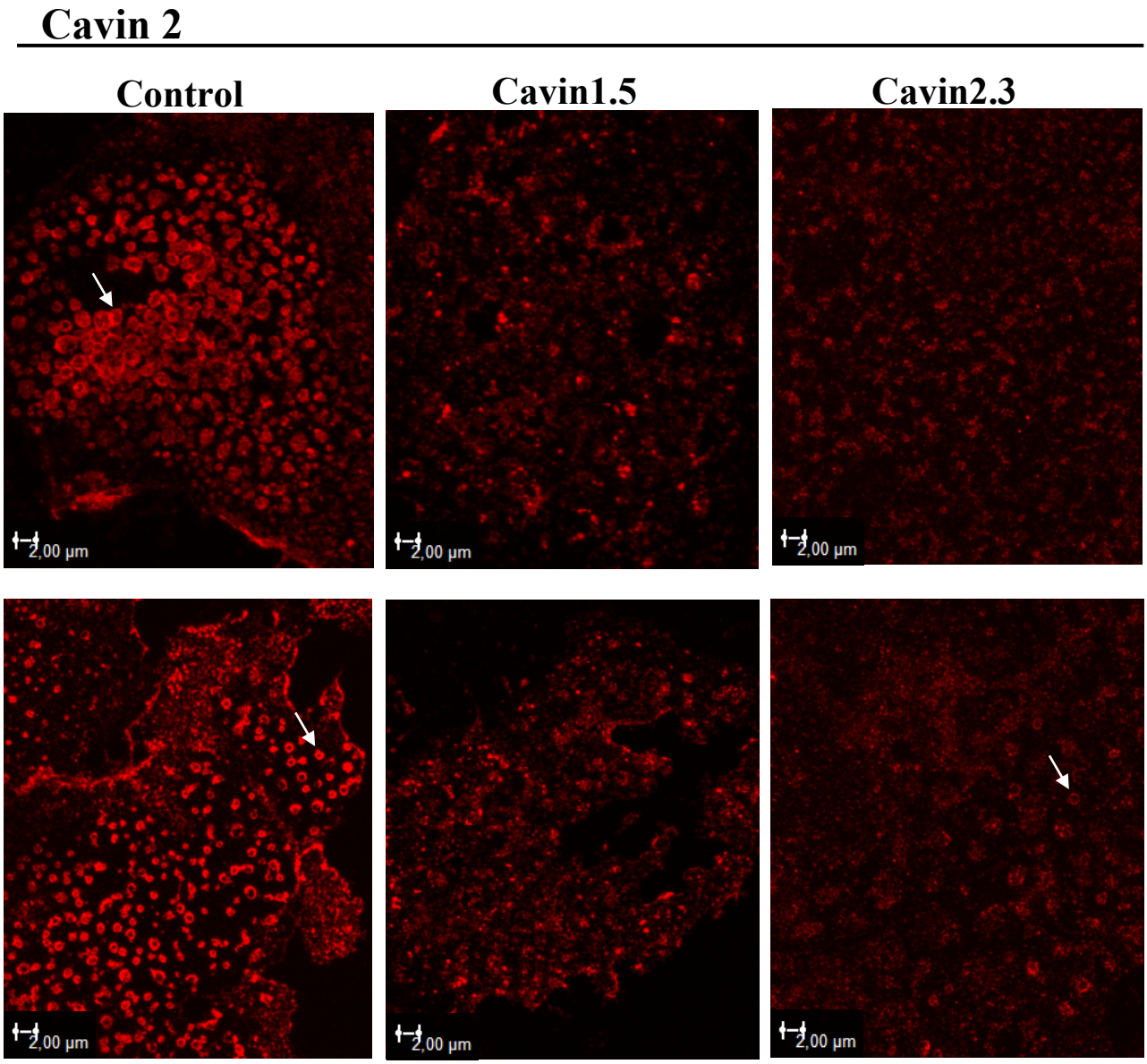

Figure 3.3 – Distribution of cavin 2 in plasma membranes of control, cavin 1 KD and cavin 2 KD cells. Control and KD adipocytes, 12 days after the induction of differentiation, were subjected to immunolocalization in plasma membrane lawns (as described in section 2.3.8 of materials and methods) using anti-cavin 2 specific antibody. Observations were made in a confocal microscope with 63x objective. Caveolae bunches are indicated by white arrows.

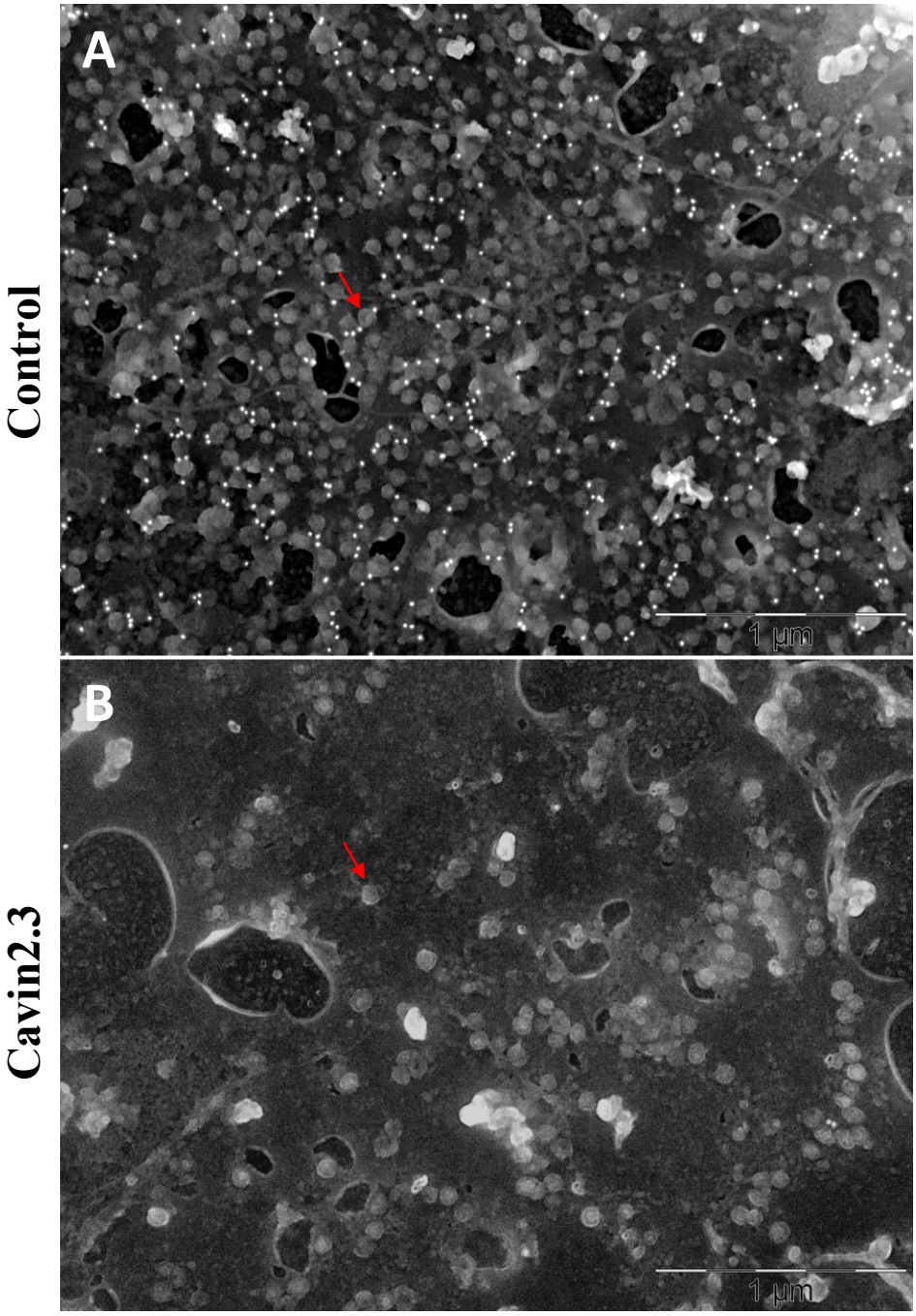

Figure 3.4 – Cavin 2 distribution in replicas of the cytosolic leaflet of the cell membrane of control (A) and cavin2.3 (B) cells. Cells in the 12th day of differentiation were processed in order to obtain plasma membrane lawns and then cavin 2 was immunolocalized using a specific antibody (as described in section 2.3.9.1 of materials and methods). Membranes were then subjected to freeze-drying technique (as described in section 2.3.9.2 of materials and methods) and observed in an electron microscope. Arrows indicate caveolae and white dots are the gold particles associated with the secondary antibody and represent cavin 2 distribution.

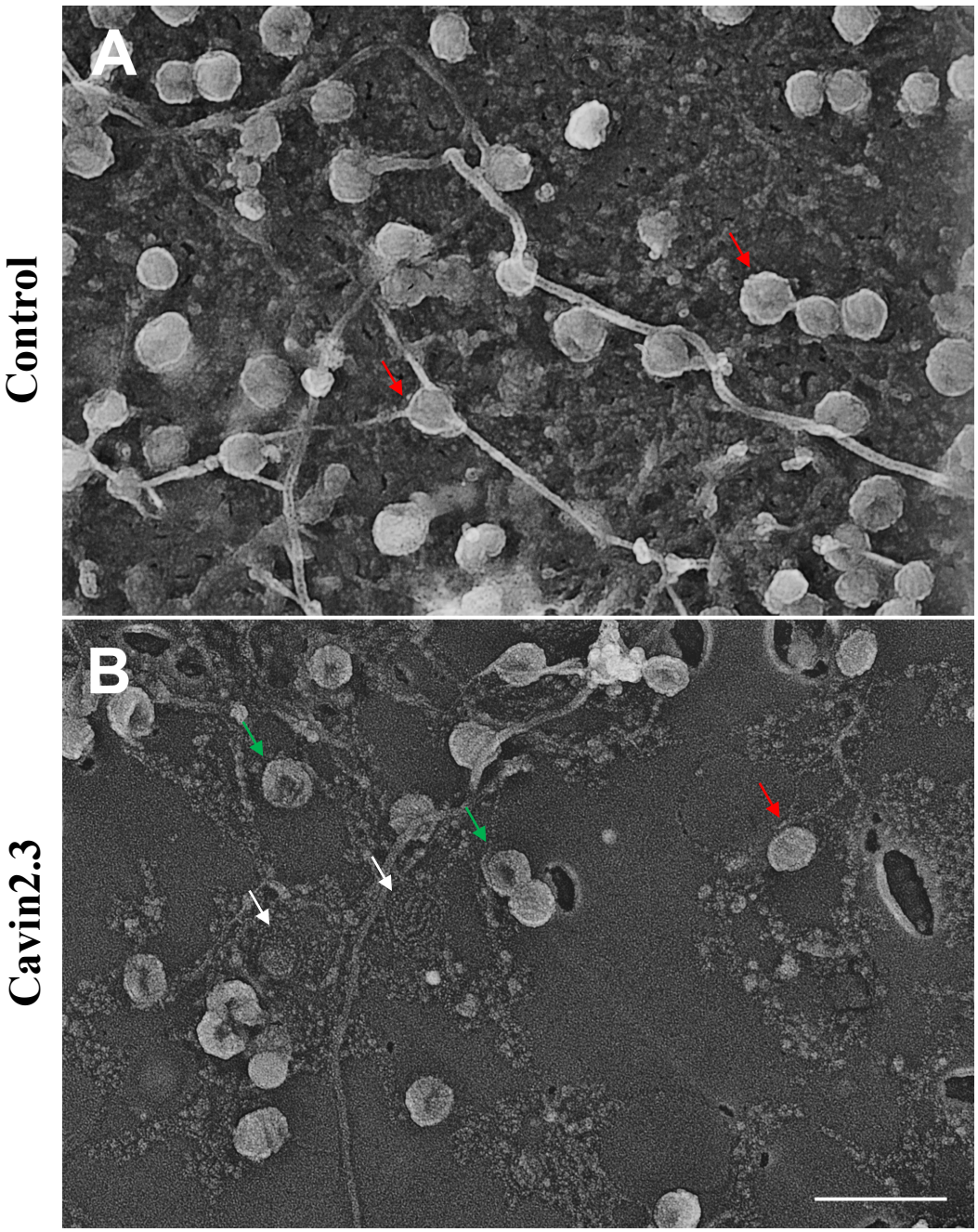

Figure 3.5 – Replicas of the cytosolic leaflet of the cell membrane of control (A) and cavin2.3 (B) cells. Cells in the 12th day of differentiation were processed in order to obtain plasma membrane lawns (as described in section 2.3.8.2 of materials and methods) and then subjected to freeze-drying technique (as described in section 2.3.9.2 of materials and methods) and observed in an electron microscope. Arrows indicate normal (red), torus shaped (green) and flattened (white) caveolae. Bar, 200nm

3.2 Differentiation of 3T3-L1 cell lines deficient in Cavin 1 and Cavin 2

After obtaining the 3T3-L1 cell lines deficient in cavin 1 and cavin 2 we wanted to analyze the capacity of these cells to differentiate. By optical microscope analysis one can evaluate the cellular differentiation analyzing the number and size of differentiated cells and its LDs. In figure 3.6, we observe that the number of differentiated cavin1.5 adipocytes is lower than the one observed in control and cavin2.3 cells, which is similar. Despite this, cavin1.5 and cavin2.3 adipocytes cells are bigger than control cells and have larger LDs. The difference in the size of LDs is clear in figure 3.6B, and because LDs store TAG we decided to quantify TAG in total lysates (figure 3.7).

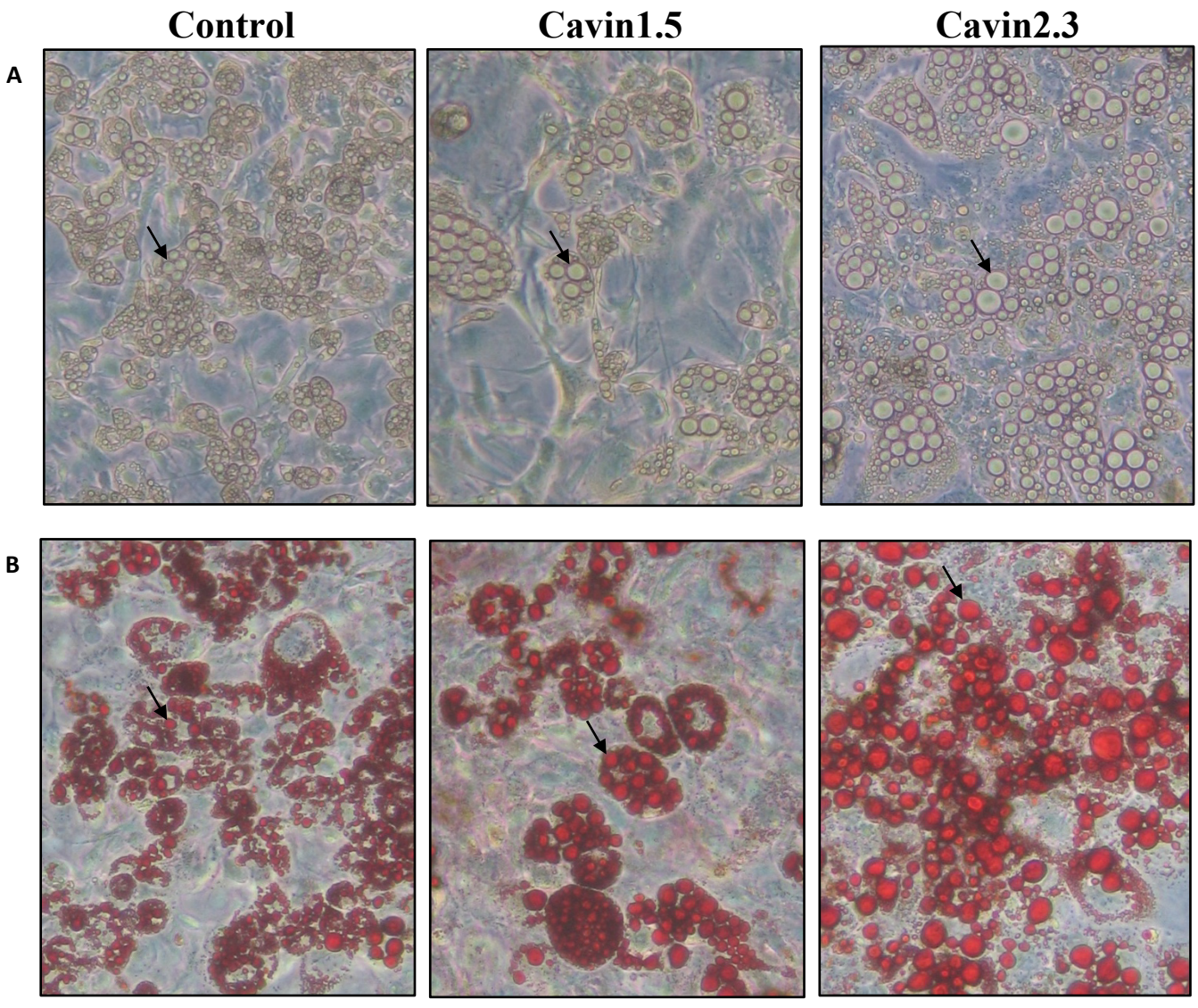

Figure 3.6 – Microscopic observation of 3T3-L1 control cells and cavin 1 and cavin 2 KD cells, not stained (A) and stained (B) with Oil Red O. A) Pre-adipocytes were induced to differentiate and 12 days after induction cells were observed in a phase contrast microscope with 10x objective. B) Adipocytes in the 12th day of differentiation were fixed and stained with Oil Red O (as described in section 2.3.10 of materials and methods) and observed in a phase contrast microscope with 10x objective. LDs are indicated by black arrows.

In this quantification we observe that the level of TAG in cavin2.3 cells is higher than in control cells but this difference is not significative, on the other hand TAG levels are lower in cavin1.5 cells (around 50%). Since we quantified TAGs in total lysates and not only in differentiated cells, the fact that fewer cavin1.5 fibroblast are differentiated may account for the lower levels of TAG observed in total lysates of cavin1.5 cells.

Taken together these results indicate that cavin2.3 cells have similar differentiation profiles to those of control cells but that differentiation in cavin1.5 KD cells is affected.

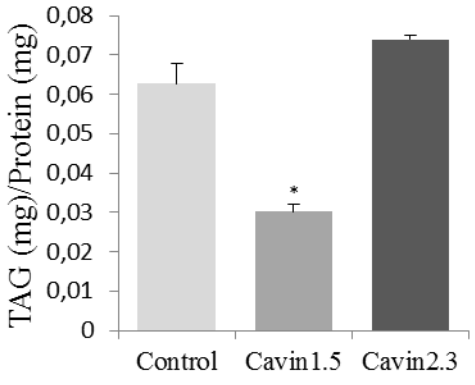

Figure 3.7 – TAG levels in total cell lysates of control, cavin1.5 and cavin2.3 cells. Control and KD adipocytes on the 12th day of differentiation were lysed and subjected to TAG quantification (as described in section 2.3.11 of materials and methods). Each data point represents the mean ±SEM derived from two independent experiments. One-way ANOVA test was performed between KD and control cells. *, P≤0,05.

To continue the analysis of the KD cells capability to differentiate we performed western blot assays to verify the expression levels of proteins markers of differentiated adipocytes such as caveolin-1, GLUT4, perilipin, ATGL, Fat acid binding protein 4 (FABP4) and IR (figure 3.8).

We verified that most of the proteins have similar expression levels. Caveolin-1 and IR levels are not altered in KD cells, although cavin1.5 has lower but not significant caveolin-1 expression. The lower levels of expression in cavin1.5 cells are also evident for ATGL and FABP4. However none of these differences are statistically relevant, as shown for caveolin-1 (figure 3.8 B). These results are consistent with the microscopic observation where cavin1.5 cells show a worst differentiation profile.

On other hand, levels of GLUT4 and perilipin are altered in KD cells. GLUT4 protein levels showed a decrease of 89% in cavin1.5 cells and 47% in cavin2.3 when compared with control cells (figure 3.8 B). Expression level of perilipin it is decreased in cavin1.5 cells (around 55% less) and increased in cavin2.3 cells but this difference is not statistically relevant (figure 3.8 B).

Considering that cavin1.5 cells have lower percentage of differentiated adipocytes and that we analyzed total lysates, it is not surprising that the expression levels of these differentiation markers is lower than that of control cells.

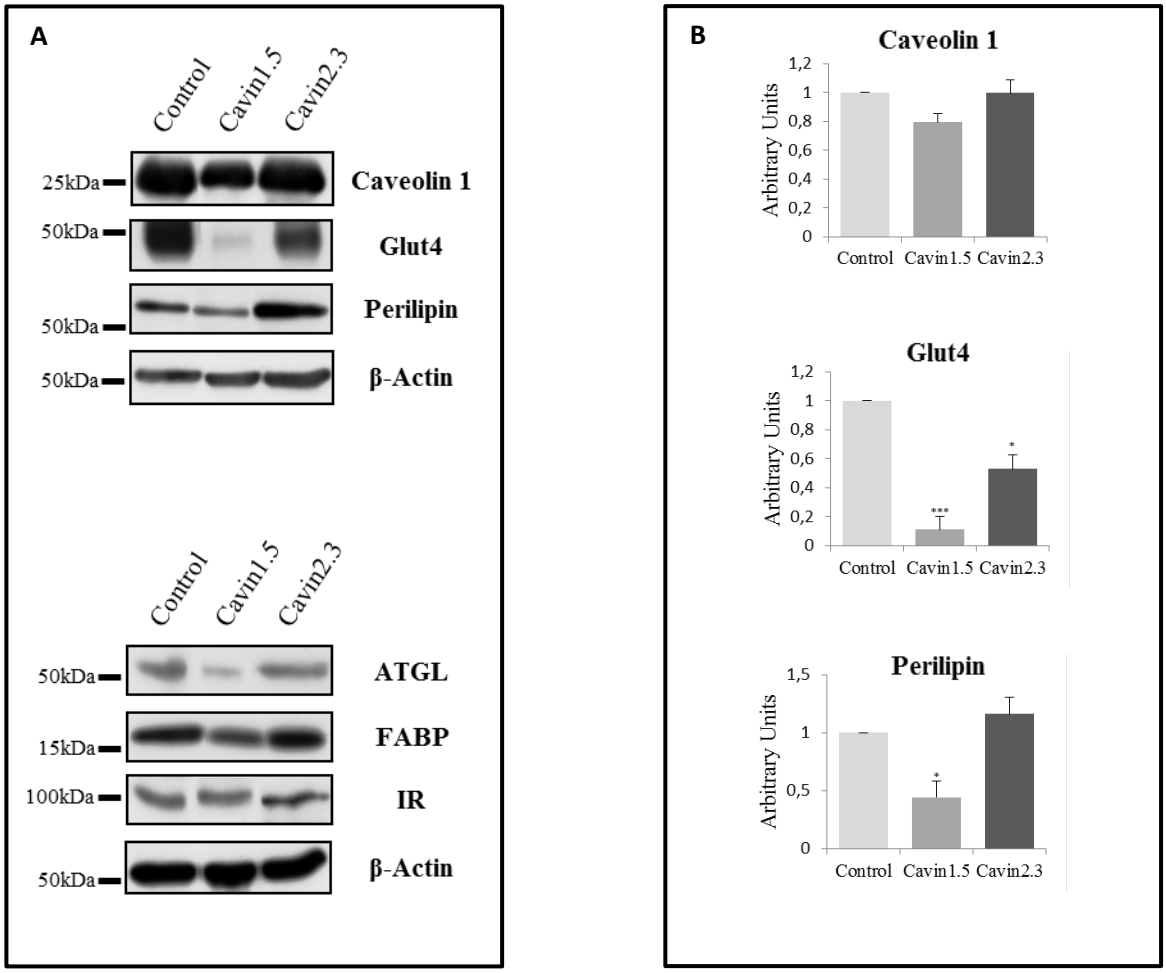

Figure 3.8 – Expression levels of protein markers of adipocyte differentiation in control and KD cells. A) 3T3-L1 control cells and KD cells were lysed 12 days after the induction of adipocyte differentiation and 50µg of cell lysates (5µg for caveolin-1 and GLUT4) were resolved by SDS-PAGE and analyzed by western blot with specific antibodies for protein markers of adipocyte differentiation. B) Quantification of western blot bands obtained for caveolin-1, GLUT4 and perilipin. Each data point represents the mean ±SEM derived from independent experiments (six for caveolin-1 and perilipin and five for GLUT4) normalized to control cells. One-way ANOVA test was performed between KD and control cells. ***, P≤0,001; *, P≤0,05.

As previously referred, cavins are present in plasma membrane domains called caveolae, these structures are enriched in caveolin-1 which is its more abundant protein. Since levels of caveolin-1 in total lysates are similar in control and KD cells we decided to immunolocalize caveolin-1 in plasma membrane lawns of differentiated adipocytes in order to observe if caveolin-1 distribution is normal and to analyze caveolae structure. In figure 3.9 and 3.10 one observes that KD cells have less caveolin-1 in the plasma membrane than control cells, however, in figure 3.9 this is not so obvious for cavin2.3 cells since the images have a lot of background signal which could be confused with caveolin signal. As for the structure of caveolae, like observed with anti-cavin 2 antibody (figure 3.3 and 3.4), caveolae are altered/absent in both KD cells. Comparing these results with the ones in figure 3.3, 3.4 and 3.5 it seems that lack of cavins affects with great extent caveolae formation.

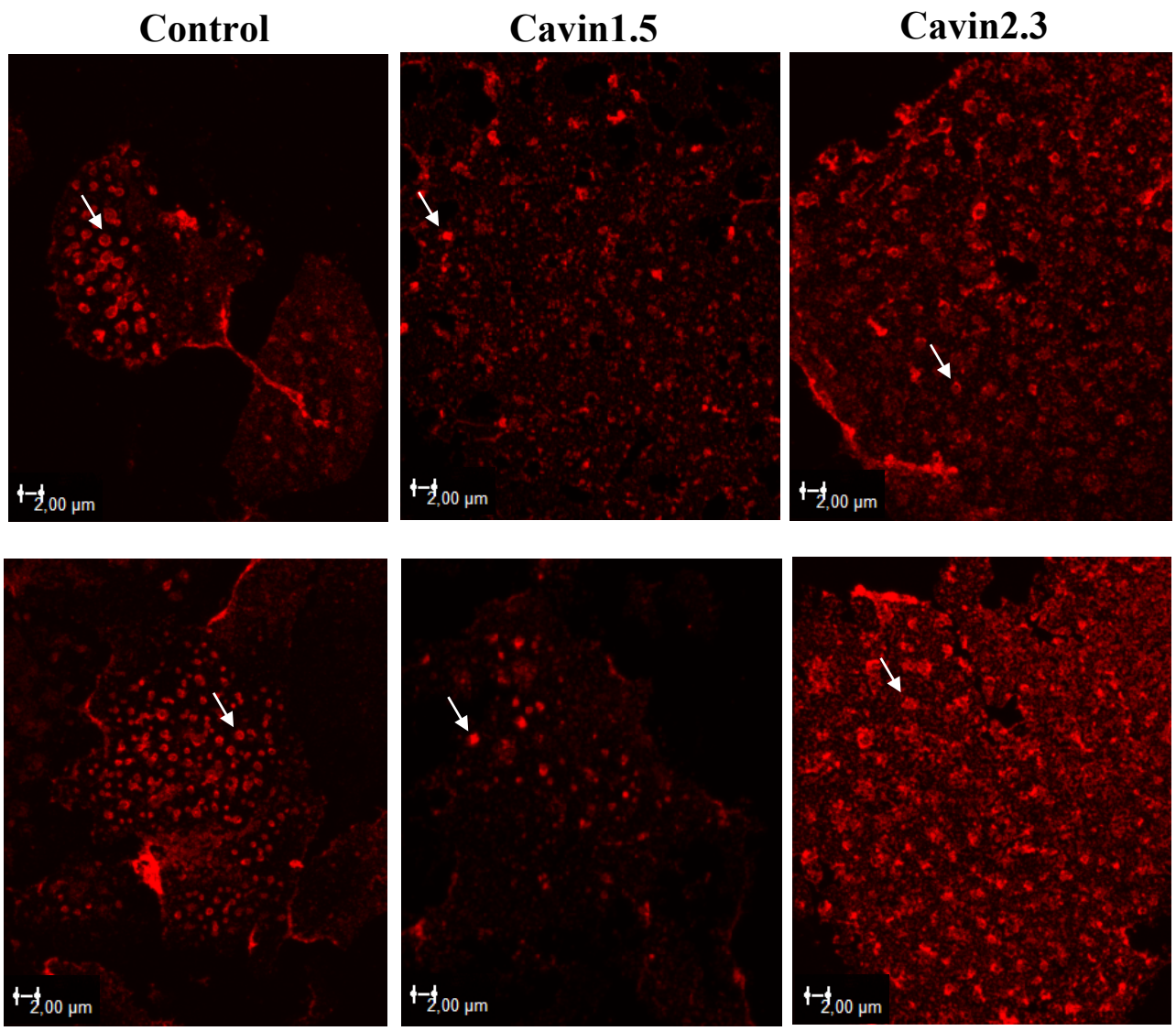

Figure 3.9 – Distribution of caveolin-1 in plasma membranes (cytosolic leaflet) of control and KD cells. Control and KD adipocytes, 12 days after the induction of differentiation, were processed in order to obtain plasma membrane lawns and caveolin-1 was immunolocalized with a specific antibody (as described in section 2.3.8 of materials and methods). Observations were made in a confocal microscope with 63x objective. Caveolae are indicated by white arrows.

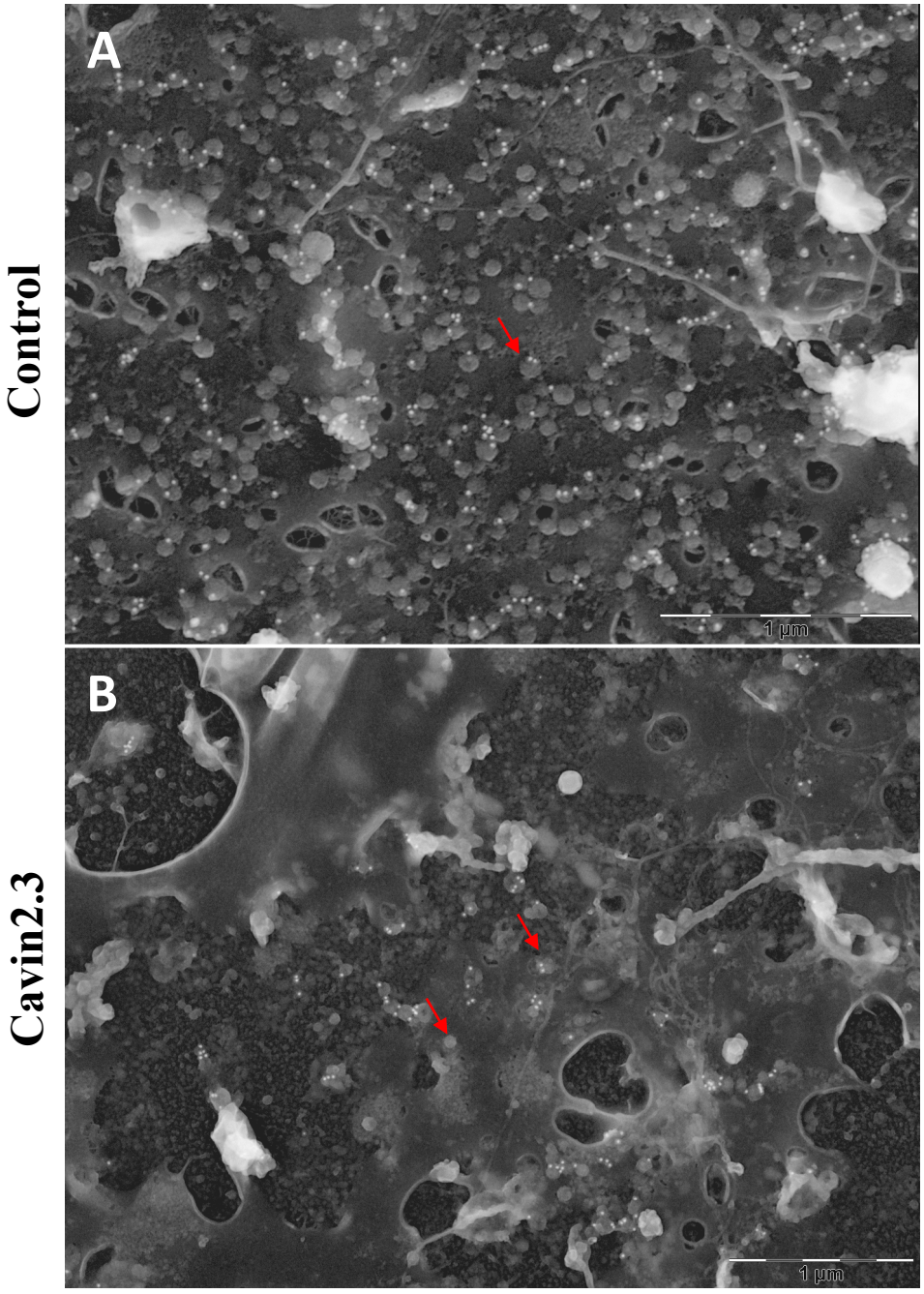

Figure 3.10 – Caveolin-1 distribution in replicas of the cytosolic leaflet of the cell membrane of control (A) and cavin2.3 (B) cells. Cells in the 12th day of differentiation were processed in order to obtain plasma membrane lawns and then cavolin-1 was immunolocalized using a specific antibody (as described in section 2.3.9.1 of materials and methods). Membranes were then subjected to freeze-drying technique (as described in section 2.3.9.2 of materials and methods) and observed in an electron microscope. Red arrows indicate caveolae and white dots represent caveolin-1 distribution.

Perilipin is one of the most abundant proteins in the membrane of LDs and in order support the previous observation about LDs size and perilipin content we performed an immunolocalization of perilipin in control and KD cells (figure 3.11). The immunolocalization allowed us to confirm that KD cells have bigger LDs than control cells, however we could not observe any differences in the amount of this protein.

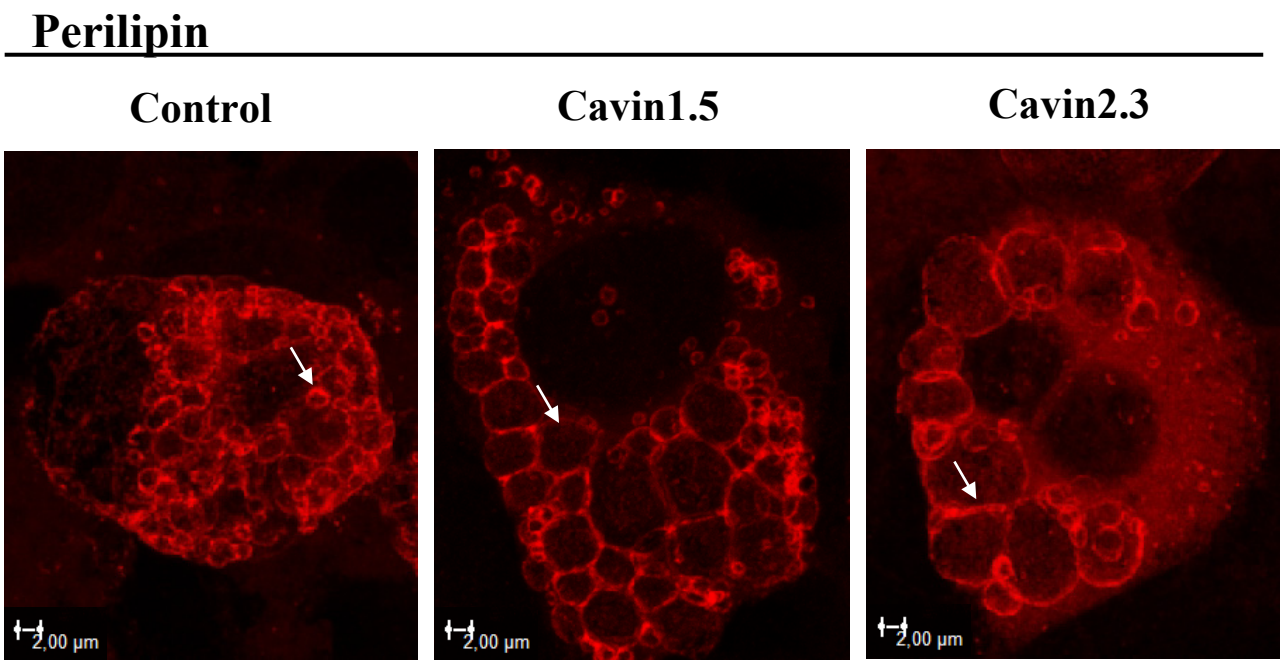

Figure 3.11 – Distribution of perilipin in LDs of control and KD cells. Control and KD adipocytes, 12 days after the induction of differentiation, were subjected to immunolocalization in whole-cells (as described in section 2.3.8 of materials and methods) using anti-perilipin antibody. Observations were made in a confocal microscope with 63x objective. LDs containing perilipin in its surface are indicated by white arrows.

3.3 Insulin responsiveness of 3T3-L1 cell lines deficient in Cavin 1 and Cavin 2

GLUT4 is the insulin-regulated glucose transporter found in adipose tissues and since the levels of this transporter are reduced in KD cells we decided to evaluate the ability of these cells to transport glucose in response to insulin.

Analyzing the insulin-responsive transport of cavin2.3 cells (figure 3.12 A) one observes that these cells only respond to insulin at a concentration of 10nM while control cells respond at 1nM. At 10nM already exists a significant difference between control and cavin2.3 cells and this difference increases at 100nM insulin. Summarizing, KD cells are less insulin-sensitive because they need higher insulin concentration (than control cells) to increase glucose transport and the response to the hormone is less effective because glucose uptake at 10nM and specially at 100nM of insulin is significantly lower in cavin2.3 cells.

Regarding cavin1.5 cells responsiveness to insulin (figure 3.12 B) we observed that these KD cells do not respond to any of the insulin concentrations used in this experiment, which is not surprising considering that cavin1.5 cells have low levels of GLUT4. Apart from the cavin 1 KD cells unresponsiveness to insulin, we observed that the only significant difference between control and cavin 1 KD cells occurs at basal state. Cavin1.5 cells have a much higher basal transport of glucose than control cells. The higher basal uptake may result from the fact that cavin1.5 cells have less differentiated adipocytes, therefore the content of fibroblasts in the sample is high. Fibroblasts primarily use GLUT1 as a glucose transporter which is not an insulin-regulated glucose transporter and so it is not surprising that these cells have higher basal glucose transport.

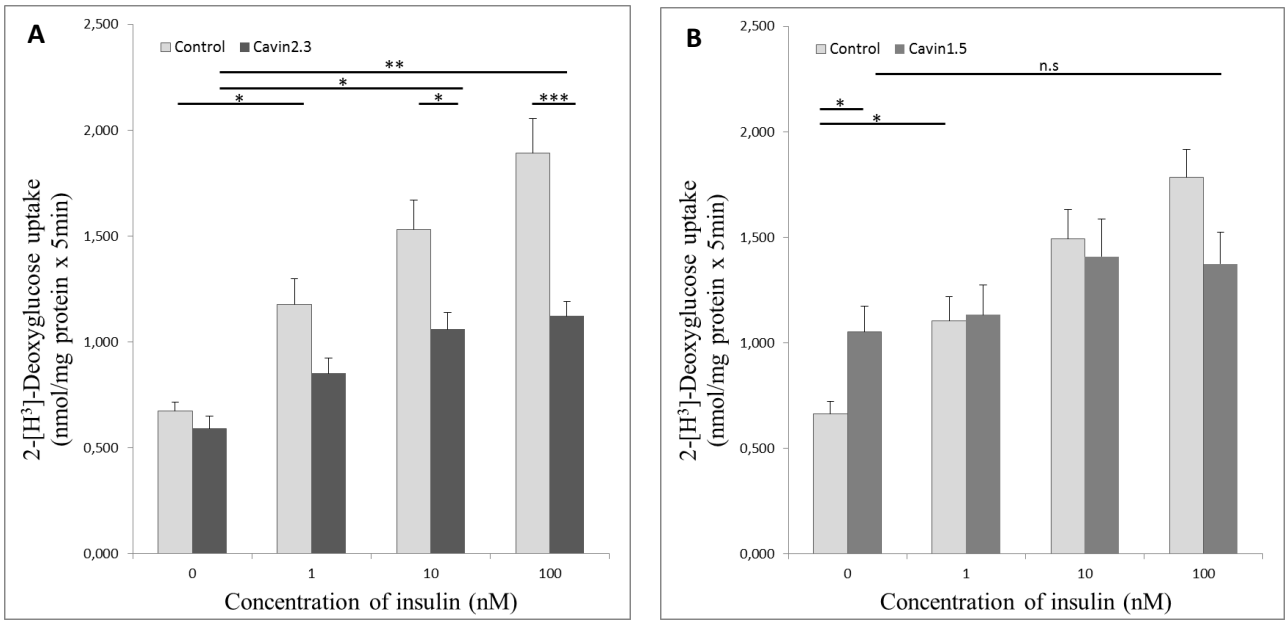

Figure 3.12 – Glucose uptake in response to different insulin concentrations by control and KD cells. Control, cavin2.3 (A) and cavin1.5 cells (B) were incubated for 30 minutes with different insulin concentrations and glucose uptake (during 5 minutes) was measured by 2-[H^3]-deoxyglucose uptake as described in materials and methods section 2.3.7. Each data point represents the mean ±SEM derived from independent experiments (nine for cavin2.3cells and eight for cavin1.5). One-way ANOVA test was performed between KD and control cells. ***, P≤0,001; **,P≤0,01; *, P≤0,05.

In order to verify if the differences observed in glucose uptake in response to insulin are caused by deficiencies in the insulin signaling pathway we performed immunoprecipitations and western blot assays to verify the levels of phosphorylated proteins involved in this signaling cascade. We analyzed expression levels of total Akt and Akt phosphorylated in serine 473, phosphotyrosine-IRS-1, phosphotyrosine-IR and PI3K (p85 subunit) linked to IRS-1. Quantifying several western blot results we obtained the graphics pictured in figure 3.13. Analyzing figure 3.13 we observe that although we see some differences between control, cavin1.5 and cavin2.3 cells, none of them are statistically significant.

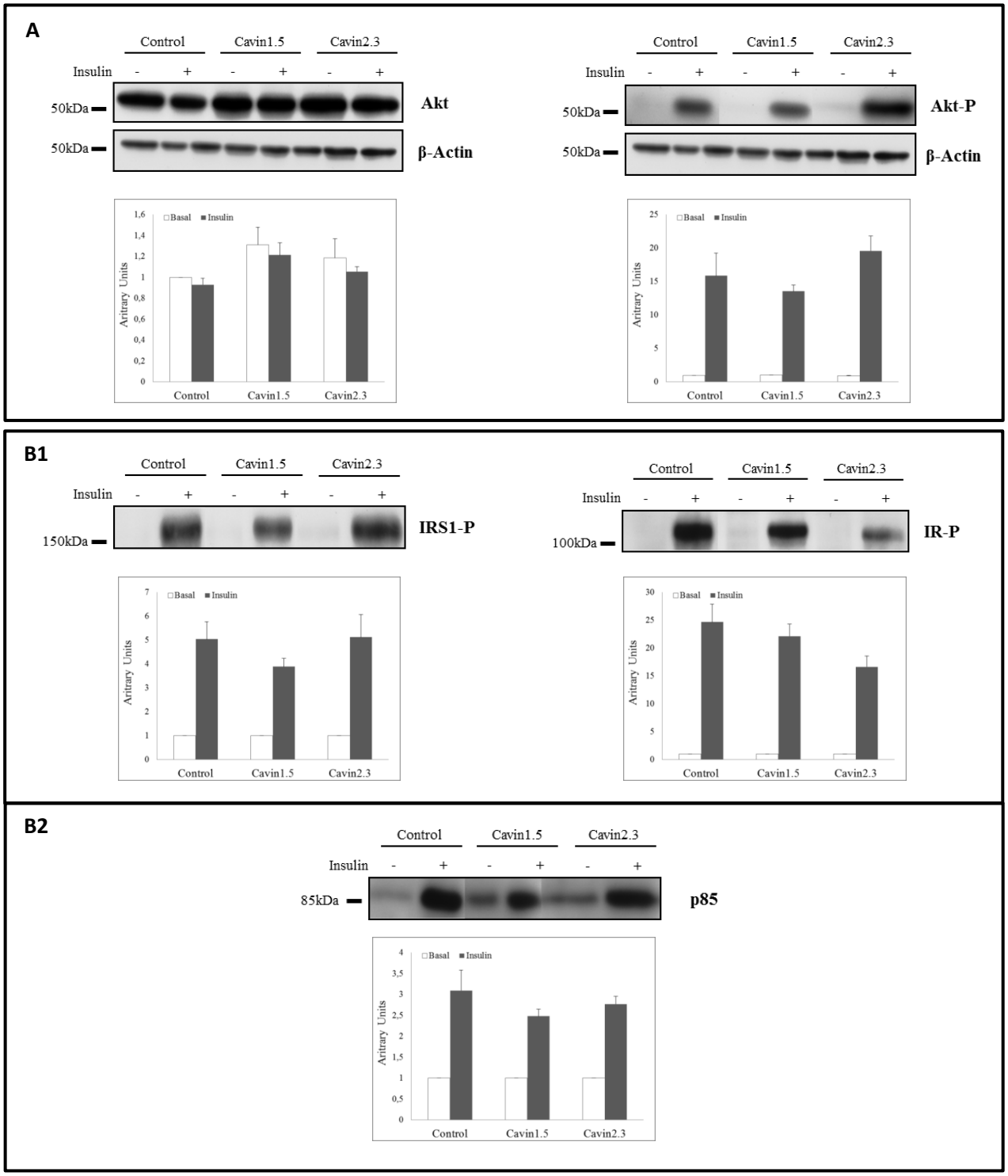

Figure 3.13 – Expression levels of phosphorylated proteins involved in the insulin signaling cascade. A) 3T3-L1 control cells and KD cells, 12 days after the induction of adipocyte differentiation, were incubated with (insulin) or without (basal) 100nM insulin for 30 minutes (as described in section 2.3.8.1 of materials and methods). Cells were lysed and 50µg of cell lysate was resolved by SDS-PAGE and analyzed by western blot with antibodies for Akt and Akt phosphorylated in serine473 (sections 2.3.3 and 2.3.5 of the methods). B) 3T3-L1 control cells and KD cells, 12 days after the induction of adipocyte differentiation, were incubated with (insulin) or without (basal) 100nM insulin for 30 minutes. Cells were lysed and 500µg of cell lysate was used for immunoprecipitation with an anti-phosphotyrosine (B1) or anti-IRS1 (B2) antibodies. Then pellets were washed and resolved by SDS-PAGE and analyzed by western blot with antibodies for IRS-1, IR (B1) and PI3K (p85 subunit) (B2) (as described in section 2.3. of materials and methods). In the quantification of western blot bands, each data point represents the mean ±SEM derived from independent experiments (Five for Akt and Akt-P; four for IR-P; three for p85 and IRS1) normalized to control cells in basal state. One-way ANOVA test was performed between KD and control cells stimulated with insulin.

Since no major differences were observed in the insulin signaling pathway we decided to analyze the translocation of GLUT4 to the membrane in response to insulin. To do so we performed an immunolocalization of GLUT4 in permeabilized whole cells and in plasma membrane lawns of differentiated adipocytes (control and KD cells) incubated with or without insulin.

Analyzing whole-cells experiments (figure 3.14) we observe that the amount of GLUT4 is higher in control cells than in KD cells, as seen by western blot (figure 3.8), and that in basal conditions (no insulin stimulation) GLUT4 localizes inside the cell in both control and KD cells. However, upon insulin stimulation GLUT4 moves to the membrane in control cells but not in KD cells.

Regarding plasma membrane lawns (figure 3.15) the same phenomenon observed in whole-cells experiments happens. In basal conditions few GLUT4 is localized at the membrane, which is normal because it is mainly inside the cell and upon insulin stimulation GLUT4 level increases in control cells but not in KD cells.

Summarizing, KD cells fail to translocate GLUT4 to the membrane in response to insulin and so this defect contributes to the lower glucose uptake after insulin stimulation.

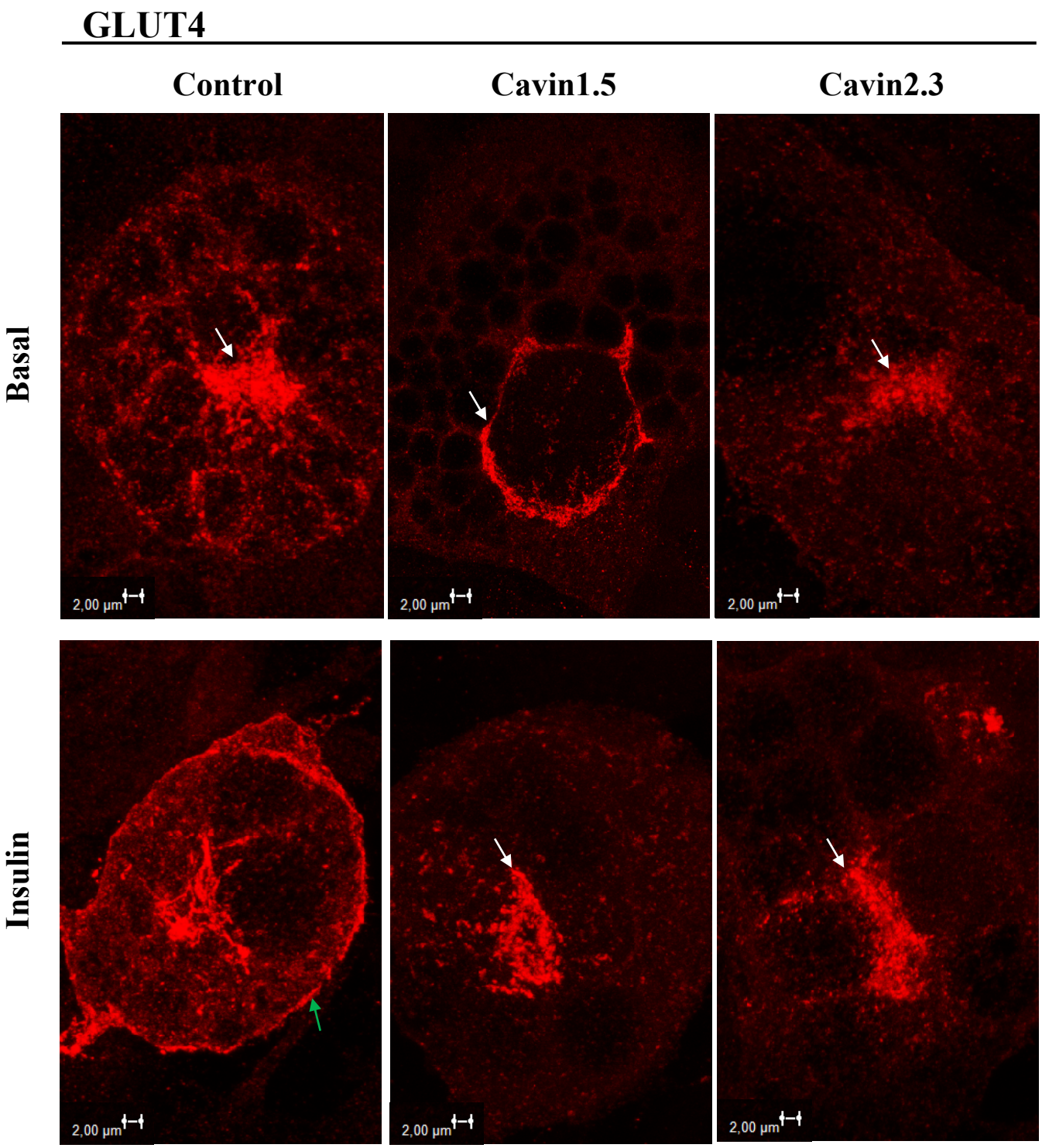

Figure 3.14 – Distribution of GLUT4 in permeabilized whole control and KD cells in the presence or absence of insulin. Control and KD adipocytes, 12 days after the induction of differentiation, were incubated with or without (basal) 100nM insulin for 30 minutes and then subjected to immunolocalization (as described in section 2.3.8 of materials and methods) using anti-GLUT4 specific antibody. Observations were made in a confocal microscope with 63x objective. GLUT4 inside the cell is indicated by white arrows and GLUT4 at the plasma membrane is indicated by green arrows.

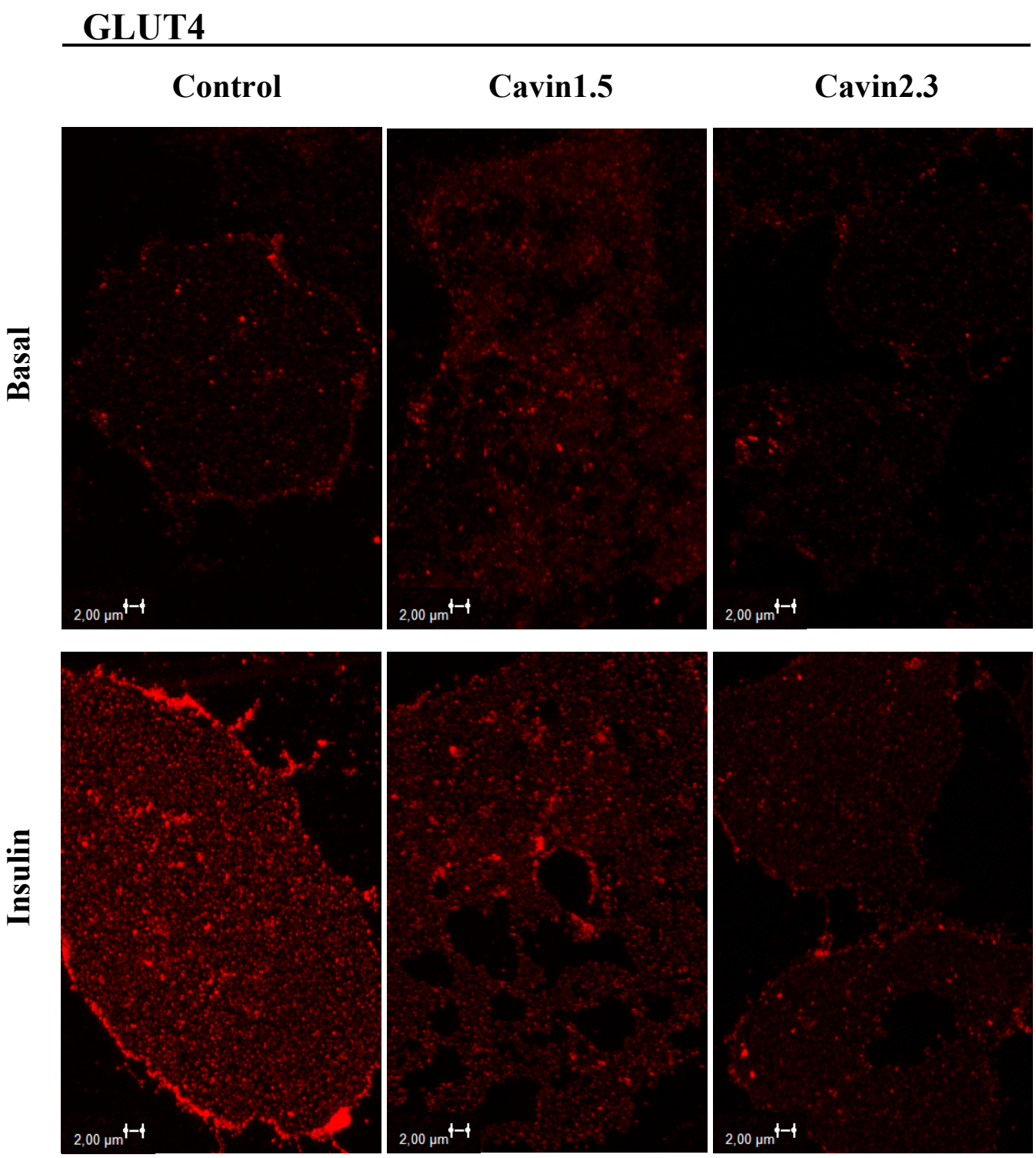

Figure 3.15 – Distribution of GLUT4 in plasma membrane lawns of control and KD cells in the presence or absence of insulin. Control and KD adipocytes, 12 days after the induction of differentiation, were incubated with or without (basal) 100nM insulin for 30 minutes. Cells were processed in order to obtain plasma membrane lawns and then subjected to immunolocalization (as described in section 2.3.8 of materials and methods) using anti-GLUT4 specific antibody. Observations were made in a confocal microscope with 63x objective.

4. Discussion

The objective of this thesis is to determine the role of the caveolar proteins, cavin 1 and cavin 2, in adipocyte functioning. To do so, we performed a siRNA-mediated KD of each protein in 3T3-L1 cell line.

Our results show that the reduction of 65% in cavin 1 expression that we obtained in the cavin 1 KD cells is sufficient to affect the differentiation of these cells.

As mentioned in the results section, the percentage of cavin 1 KD pre-adipocytes that manage to differentiate is much lower than that of control cells. However at the exception of perilipin and GLUT4, none of the differentiation markers expression was substantially reduced. In fact, the expressions of all of them were decreased but only perilipin and GLUT4 presented statistically relevant reductions. None the less, in some cases, like ATGL and FABP4, an increase in the number of experiments might be sufficient to make the protein reduction statistically relevant, since the error bars obtained in the western quantification were too high (data not shown). In cavin 1 KD cells we also observed a reduction of 48% in cavin 2 expression levels. This observation is accordant with previous results published by Bastiani *et al.* (2009) that showed a reduction in cavin 2 levels in cavin 1 3T3-L1 KD cells.

Cavin 1 KD adipocytes also presented bigger size and larger LDs (figure 3.6 and 3.11) which could explain why cavin 1 KD cells are less responsive to insulin (Le Lay *et al*., 2001). A TAG quantification in total lysates revealed that cavin 1 KD cells do not have higher TAG content despite the bigger LDs. However, as previously explained, in total lysates, the ratio of pre-adipocytes/adipocytes is higher in cavin 1 KD cells and so the TAG/protein ratio is decreased. This decrease in TAG content that we observed is also not consistent with previous studies obtained by our group (González-Muñoz *et al*., 2009) in which a KD of caveolin-1 (a protein functionally related to cavin 1) in 3T3-L1 did not affect the TAG cellular content. Thereby, we consider that the lower levels of TAG that we have quantified in cavin 1 KD cells are just a consequence of the high content of fibroblasts in the lysates. On the other hand, cavin 1 has been found in LDs, associated with caveolin-1, and has been implicated in controlling lipolysis together with HSL (Aboulaich *et al*., 2006). This suggests that the absence of cavin 1 could reduce the cell lipolytic activity, which would lead to an increase in LDs size.

Bigger LDs could also mean that cavin 1 KD cells have more perilipin, since this a component of its surface membrane, but instead, we obtained lower perilipin levels in total lysates. Immunolocalizing perilipin (figure 3.11) in whole-cells showed that there are no major differences in the LD perilipin content in differentiated control and cavin 1 KD adipocytes. Again this could be caused by the fact that less cavin 1 KD cells are induced to differentiate.

The fact that the KD of cavin 1 affected the differentiation of 3T3-L1 cells is in line with previous published results. Liu *et al*. (2008) observed that cavin 1-KO mice presented high circulating TAG levels, significantly reduced adipose tissue mass, glucose intolerance, insulin resistance and hyperinsulinemia which are all conditions of a lipodystrophic phenotype. Indeed, recently published data identified cavin 1 as a locus for human lipodystrophy (Garg, 2011; Hayashi *et al*., 2009).

Accordant with other studies (Hansen *et al*., 2009; Hill *et al*., 2008; Liu and Pilch, 2008) we observed that knocking down cavin 1 results in a reduction and morphological alteration of caveolae showing that cavin 1 is essential to this structures (figure 3.3 and 3.9). Our group (González-Muñoz *et al.,* 2009) also observed that the absence of caveolae results in a reduction at the protein level of GLUT4 (50%). This reduction was also observed in this work (figure 3.8), although in a much higher extent (89%). Part of the reduction might be due to the referred differentiation problem of the cavin 1 KD cells but it is also a consequence of the lack of cavin 1 as shown in figure 3.14.

Apart from GLUT4, our group (González-Muñoz *et al*., 2009) also observed a reduction of the IR in caveolin-1 KD adipocytes as did Liu *et al*.(2008) in cavin 1-KO mice. In our work we were not able to see this decrease. However, in both cases the models with which they work were different from ours. In Liu *et al*. (2008) the experiments were performed in a KO mice in which cavin 1 is completely absent, maybe in these conditions is possible to see the decrease in IR levels but not in ours (with 65% cavin 1 reduction). Moreover in *in vitro* experiments the culture conditions and medium are very different from those existing in *in vivo* models. In the case of González-Muñoz *et al*. (2009) the experiments were performed in 3T3-L1 cells deficient in caveolin-1 (95% reduction), not cavin 1, thereby we speculate that caveolin-1 could be more important in stabilizing IR than cavin 1. It is also a fact that in both studies the absence of caveolae was much greater than the one we observed.

Many studies have linked cavin 1 and caveolin expressions. It has been shown that in *in vivo* models the KO of cavin 1 results in a great reduction of caveolin-1 (Liu *et al*., 2008). In *in vitro* studies the same has been shown knocking down cavin 1 in 3T3-L1 cells (Hill *et al.*, 2008; Liu and Pilch, 2008). As shown in figure 3.8, we failed to do this observation. Regarding the *in vivo* experiments, the difference might be due to the same reasons we stated above for the IR expression levels. As for the Liu and Pilch (2008) model, the cavin 1 reduction they have obtained was greater than ours and this difference may be sufficient to reach a threshold where the lack of cavin 1 affects caveolin-1 levels. The importance of the cavin 1 KD percentage is evident in the work of Hill *et al.* (2008), they observed that a reduction of cavin 1 by 80-95% caused a 10-50% reduction of caveolin-1 protein levels. Moreover our results are in line with

the ones obtained by Bastiani *et al.*, 2009 in which cavin 1 KD in 3T3-L1 cells have little effect over caveolin-1 levels in total lysates.

Besides the cavin 1 KD, we also obtained a cavin 2 KD cell line. In contrast with the first, the differentiation of cavin 2 KD cells was not affected by the absence of this protein (97% reduction). Cavin 2 KD adipocytes presented a similar morphology to that of cavin 1 KD adipocytes, which means bigger cells and LDs when comparing with control cells. These differences are even more evident in cavin 2 KD cells than in cavin 1 KD cells (figure 3.6 and 3.11). Again, this is characteristic of cells with reduced insulin sensitivity (Le Lay *et al*., 2001). In the case of cavin 2 KD cells, TAGs quantification and perilipin protein levels in total lysates (figure 3.7 and 3.8) were slightly higher than those of control cells, but these differences were not statistically significant. However, these observations are accordant with the fact that cavin 2 KD cells have bigger LDs. Besides the reduction in GLUT4 levels, which will be discussed later, the expression of all the differentiations markers analyzed was not altered, thereby our results suggest that cavin 2 is not essential for adipocyte differentiation.

As observed for the cavin 1 KD cells, the reduction of the expression of cavin 2 also resulted in a reduction of cavin 1. This means that cavin 1 and 2 have interdependent expressions as previously shown (Bastiani *et al*., 2009). Pilch group, in non-published data has even observed that in cavin 2 KD cells cavin 1 is redistributed to the cytosol. We have not confirmed this observation because we could not perform cavin 1 immunolocalization experiments. Analyzing the percentages of reduction in cavin 1 and cavin 2 expressions we can assume that cavin 1 KD has a greater effect in cavin 2 expression than the reverse.

In previous studies (Bastiani *et al*., 2009; Hansen *et al*., 2009) cavin 2 was localized in caveolae and considered essential for its morphology. Our results also show that cavin 2 localizes in caveolae and that caveolae number is decreased in cavin 2 KD cells (figure 3.3, 3.4, 3.5 and 3.9), supporting the previous studies. Other works have revealed that the KD of cavin 2 in HeLa cells leads to a decrease in the levels of the most studied caveolar protein, caveolin-1. On the other hand Bastiani *et al.*(2009) have also performed a KD of cavin 2 in 3T3-L1 and they did not found a significant reduction in the caveolin-1 levels. Our results are in agreement with Bastiani's since we did not see any differences in caveolin-1 levels in total lysates but we did see a reduction in the plasma membrane. So the question is, where is caveolin-1? It has been described that caveolin-1 is present in LDs although its role in this location is still unclear (Blouin *et al*., 2008; Robenek *et al.*, 2010). Moreover, it was previously observed that the size in LD increases with the content of caveolin in the same (in obese rodent models and human adipocytes) (Blouin *et al*., 2010), thereby it is possible that caveolin-1 is localizing in the

surface of LDs in both cavin KD adipocytes, where it would be stable. One should immunolocalize caveolin-1 in whole-cells to determine the localization of this protein.

As happened with cavin 1 KD, the downregulation of cavin 2 leads to the loss of caveolae and consequently to a decrease in GLUT4 levels, which is in agreement with González-Muñoz *et al*. (2009) experiments. We obtained a 47% decrease in GLUT4 levels as did González-Muñoz with a caveolin-1 deficient 3T3-L1 cell line. However, despite the absence of caveolae, we could not see differences in the levels of IR, neither with cavin 2 nor cavin 1 KD. Since we did not observe any differences in total caveolin-1 levels, we speculate that not only caveolae but also caveolin are directly related with IR stabilization in the membrane and so, the caveolin which is still present in the membrane of our cells might be enough to stabilize the IR.

Our results also showed that the ability of cavin 1 and cavin 2 KD cells to respond to insulin increasing glucose transport is impaired (figure 3.12).

In cavin 1 KD cells we observed that there is no significant increase in the glucose uptake in response to insulin, which is not surprising considering the reduction in GLUT4 levels, the main insulin-responsive glucose transporter (figure 3.8). This inability to respond to insulin is in line with the results obtained by Pilch group in which cavin 1 KO lipodystrophic mice presented insulin resistance and hyperinsulinemia (Liu *et al*., 2008). Our results also showed a high basal glucose uptake in cavin 1 KD cells but, has previously referred, this is due to the high fibroblast content in the samples. Pre-adipocytes have a high basal glucose uptake due to high expression of GLUT1 (Yeh *et al.*, 1995).

In contrast to cavin 1, cavin 2 KD cells responded to insulin, however this insulin action was 60% lower than that of control cells. Similar results were obtained in previous works of our group. González-Muñoz *et al.* (2009) obtained a 50% reduction in glucose uptake by cells lacking caveolin-1 which also had 50% less GLUT4 while we obtained a reduction of 60% in glucose uptake by cells with 50% less GLUT4. Our results also showed that cavin 2 KD cells were less insulin-sensitive since we needed a higher insulin concentration to increase glucose uptake.

In both KD cells, the impaired increase in glucose transport induced by insulin is not surprising considering the GLUT4 levels, however our results revealed that this is not the only reason. Immunolocalizing GLUT4 in whole cells and plasma membrane lawns, after insulin stimulation, revealed that this transporter was not being translocated to the plasma membrane (figure 3.14 and 3.15). This could be caused by an alteration in the insulin-signaling pathway, however we did not detect any significant difference in the signaling cascade (figure 3.13), although Liu *et al*. (2008) reported a reduction in phosphorylated Akt levels (phosphorylation in ser473) in cavin 1 KO mice. As previously discussed, this can be a consequence of the

differences that exist between *in vivo* and *in vitro* experiments. On the other hand, González-Muñoz *et al*. (2009) did not found any changes in the insulin cascade in caveolin-1 deficient adipocytes. Some key points in this pathway, like AS160 and PKCζ, were not analyzed, thus this is something one needs to do in order to understand if this inability to translocate GLUT4 results from a flawed in the insulin-signaling cascade.

If signaling pathway is normal, the impaired GLUT4 translocation can be either due to a mislocation of GLUT4, meaning that the transporter is not localized to de GSVs, or to some alteration in the mechanisms that lead to the movement and fusion of the GSVs with the plasma membrane. To test these possibilities it is important to co-localize GLUT4 with other GSVs markers or with markers of recycling endosomes (RE) which also contain GLUT4 and that are thought to be involved in the recycling that the transporter undergoes in the absence of insulin. Usually GSVs and RE are distinguished by the presence of the transferrin receptor, which is present in RE but not in GSVs (Zaid *et al.,* 2008; Lamb *et al.,* 2010). Recent studies propose that these two vesicles populations can also be distinguished through the content in Vesicle-Associated Membrane Protein (VAMP) fusion proteins, it has been hypothesized that GSVs possess VAMP2 and RE, VAMP7 (Zaid *et al.,* 2008). Apart from verifying if GLUT4 is in the GVSs it would be important to check for Golgi-localized, γ-ear-containing, Arf (ADP-ribosylation factor)-binding protein (GGA) levels. Watson *et al*. (2004) observed that expression of a dominant-interfering GGA mutant completely blocked the insulin-stimulated translocation of newly synthetized GLUT4, and established GGA as an indispensable protein in the sorting of GLUT4 into the GSVs. Therefore, an alteration in GGA could explain the results obtained in this work. Previously, we referred that is important to analyze AS160, this analysis is important not only because AS160 is a component of the insulin signaling cascade but also because it regulates the movement of GSVs to the membrane. Phosphorylation of this protein is central for the stabilization of its targets, Rab proteins, in the GTP-bound form, which are thought to promote vesicles traffic (Klip, 2009; Rowland *et al.*, 2011; Watson and Pessin, 2006).

Understanding the reason why cavin 1 and cavin 2 KD cells fail to deliver GLUT4 to the membrane is not an easy task since the link between insulin signaling cascade and GLUT4 translocation to the membrane is not fully understood and because up to date no connection between cavins and GSVs trafficking has been made, thereby we think this work is the beginning of a journey.

Putting all the results together we confirmed that both cavin 1 and cavin 2 localize in caveolae, that they are needed for caveolae formation and that cavin 1 and cavin 2 expression levels are dependent on each other. We concluded that cavin 1 is necessary for adipocyte differentiation and that both cavin 1 and cavin 2 affect GLUT4 protein levels. Finally, we

concluded that cavin 1 and cavin 2 are necessary for insulin-stimulated GLUT4 translocation to the plasma membrane and for insulin-stimulated glucose transport.

To continue this work we aim to identify or characterize the compartments where GLUT4 is being held in cavin KD cells, as said above, immunolocalizing transferrin receptor and VAMP proteins and we also want to verify the levels of GGA and AS160 which are essential in the GLUT4 sorting to the GSVs and to translocate these vesicles to caveolae, respectively. It is also important to examine the location of caveolin-1, verifying by immunolocalization if caveolin-1 is present in the LDs as we hypothesized. Finally, we want to characterize KD cells when differentiated in low glucose medium, in an attempt to reach more physiological conditions.

5. References

- Aboulaich, N., Ortegren, U., Vener, A. V. and Stralfors, P. 2006. Association and insulin regulated translocation of hormone-sensitive lipase with PTRF. Biochem Biophys Res Commun 350: 657-661.

- Aronoff, S.L., Berkowitz, K., Shreiner, B. and Want, L. 2004. Glucose Metabolism and Regulation: Beyond Insulin and Glucagon. Diabetes Spectrum 17:183-91.

- Bastiani, M., Liu, L., Hill, M. M., Jedrychowski, M. P., Nixon, S. J., Lo, H. P., Abankwa, D., Luetterforst, R., Fernandez-Rojo, M., Breen, M. R., Gygi, S. P., Vinten, J., Walser, P. J., North, K. N., Hancock, J. F., Pilch, P. F. and Parton, R. G. 2009. MURC/Cavin-4 and cavin family members form tissue-specific caveolar complexes. J Cell Biol 185: 1259-1273.

- Bellacosa, A., Testa, J. R., Moore, R. and Larue, L. 2004. A portrait of AKT kinases: human cancer and animal models depict a family with strong individualities. Cancer Biol Ther 3: 268-275.

- Bickel, P. E., Tansey, J. T. and Welte, M. A. 2009. PAT proteins, an ancient family of lipid droplet proteins that regulate cellular lipid stores. Biochim Biophys Acta 1791: 419-440.

- Blouin, C. M., Le Lay, S., Lasnier, F., Dugail, I. and Hajduch, E. 2008. Regulated association of caveolins to lipid droplets during differentiation of 3T3-L1 adipocytes. Biochem Biophys Res Commun 376: 331-335.

- Blouin, C. M., Le Lay, S., Eberl, A., Kofeler, H. C., Guerrera, I. C., Klein, C., Le Liepvre, X., Lasnier, F., Bourron, O., Gautier, J. F., Ferre, P., Hajduch, E. and Dugail, I. 2010. Lipid droplet analysis in caveolin-deficient adipocytes: alterations in surface phospholipid composition and maturation defects. J Lipid Res 51: 945-956.

- Boura-Halfon, S. and Zick, Y. 2009. Phosphorylation of IRS proteins, insulin action, and insulin resistance. Am J Physiol Endocrinol Metab 296: E581-591.

- Briand, N., Dugail, I. and Le Lay, S. 2010. Cavin proteins: New players in the caveolae field. Biochimie.

- Brown, D. A. 2001. Lipid droplets: proteins floating on a pool of fat. Curr Biol 11: R446-449.

- Bryant, N. J., Govers, R. and James, D. E. 2002. Regulated transport of the glucose transporter GLUT4. Nat Rev Mol Cell Biol 3: 267-277.

- Campbell, R. K. 2009. Type 2 diabetes: where we are today: an overview of disease burden, current treatments, and treatment strategies. J Am Pharm Assoc (2003) 49 Suppl 1: S3-9.

- Chadda, R. and Mayor, S. 2008. PTRF triggers a cave in. Cell 132: 23-24.

- Choi, K. and Kim, Y. B. 2010. Molecular mechanism of insulin resistance in obesity and type 2 diabetes. Korean J Intern Med 25: 119-129.

- Cohen, A. W., Razani, B., Schubert, W., Williams, T. M., Wang, X. B., Iyengar, P., Brasaemle, D. L., Scherer, P. E. and Lisanti, M. P. 2004. Role of caveolin-1 in the modulation of lipolysis and lipid droplet formation. Diabetes 53: 1261-1270.

- Costacou, T. and Mayer-Davis, E. J. 2003. Nutrition and prevention of type 2 diabetes. Annu Rev Nutr 23: 147-170.

- Dandekar, A. A., Wallach, B. J., Barthel, A. and Roth, R. A. 1998. Comparison of the signaling abilities of the cytoplasmic domains of the insulin receptor and the insulin receptor-related receptor in 3T3-L1 adipocytes. Endocrinology 139: 3578-3584.

- DeFronzo, R. A. and Tripathy, D. 2009. Skeletal muscle insulin resistance is the primary defect in type 2 diabetes. Diabetes Care 32 Suppl 2: S157-163.

- Doornbos, R. P., Theelen, M., van der Hoeven, P. C., van Blitterswijk, W. J., Verkleij, A. J. and van Bergen en Henegouwen, P. M. 1999. Protein kinase Czeta is a negative regulator of protein kinase B activity. J Biol Chem 274: 8589-8596.

- Ducharme, N. A. and Bickel, P. E. 2008. Lipid droplets in lipogenesis and lipolysis. Endocrinology 149: 942-949.

- Engelman, J. A., Lee, R. J., Karnezis, A., Bearss, D. J., Webster, M., Siegel, P., Muller, W. J., Windle, J. J., Pestell, R. G. and Lisanti, M. P. 1998. Reciprocal regulation of neu tyrosine kinase activity and caveolin-1 protein expression in vitro and in vivo. Implications for human breast cancer. J Biol Chem 273: 20448-20455.

- Farese, R. V. 2002. Function and dysfunction of aPKC isoforms for glucose transport in insulin-sensitive and insulin-resistant states. Am J Physiol Endocrinol Metab 283: E1-11.

- Forcheron, F., Legedz, L., Chinetti, G., Feugier, P., Letexier, D., Bricca, G. and Beylot, M. 2005. Genes of cholesterol metabolism in human atheroma: overexpression of perilipin and genes promoting cholesterol storage and repression of ABCA1 expression. Arterioscler Thromb Vasc Biol 25: 1711-1717.

- Friedman, J. 2002. Fat in all the wrong places. Nature 415: 268-269.

- Garg, A. 2011. Lipodystrophies: Genetic and Acquired Body Fat Disorders. J Clin Endocrinol Metab.

- Gonzalez-Munoz, E. 2007. Papel de las caveolas/caveolina-1 en la fisiología del adipocito. PhD Thesis. Faculty of Biology, University of Barcelona.

- Gonzalez-Munoz, E., Lopez-Iglesias, C., Calvo, M., Palacin, M., Zorzano, A. and Camps, M. 2009. Caveolin-1 loss of function accelerates glucose transporter 4 and insulin receptor degradation in 3T3-L1 adipocytes. Endocrinology 150: 3493-3502.

- Guillausseau, P. J., Meas, T., Virally, M., Laloi-Michelin, M., Medeau, V. and Kevorkian, J. P. 2008. Abnormalities in insulin secretion in type 2 diabetes mellitus. Diabetes Metab 34 Suppl 2: S43-48.

- Hansen, C. G., Bright, N. A., Howard, G. and Nichols, B. J. 2009. SDPR induces membrane curvature and functions in the formation of caveolae. Nat Cell Biol 11: 807-814.

- Hansen, C. G. and Nichols, B. J. 2010. Exploring the caves: cavins, caveolins and caveolae. Trends Cell Biol 20: 177-186.

- Hayashi, Y. K., Matsuda, C., Ogawa, M., Goto, K., Tominaga, K., Mitsuhashi, S., Park, Y. E., Nonaka, I., Hino-Fukuyo, N., Haginoya, K., Sugano, H. and Nishino, I. 2009. Human PTRF mutations cause secondary deficiency of caveolins resulting in muscular dystrophy with generalized lipodystrophy. J Clin Invest 119: 2623-2633.

- Hayer, A., Stoeber, M., Bissig, C. and Helenius, A. 2010. Biogenesis of caveolae: stepwise assembly of large caveolin and cavin complexes. Traffic 11: 361-382.

- Hill, M. M., Bastiani, M., Luetterforst, R., Kirkham, M., Kirkham, A., Nixon, S. J., Walser, P., Abankwa, D., Oorschot, V. M., Martin, S., Hancock, J. F. and Parton, R. G. 2008. PTRF-Cavin, a conserved cytoplasmic protein required for caveola formation and function. Cell 132: 113-124.

- Huang, S. and Czech, M. P. 2007. The GLUT4 glucose transporter. Cell Metab 5: 237-252.

- Huang, X. F. and Chen, J. Z. 2009. Obesity, the PI3K/Akt signal pathway and colon cancer. Obes Rev 10: 610-616.

- Karlsson, M., Thorn, H., Parpal, S., Stralfors, P. and Gustavsson, J. 2002. Insulin induces translocation of glucose transporter GLUT4 to plasma membrane caveolae in adipocytes. FASEB J 16: 249-251.

- Klip, A. 2009. The many ways to regulate glucose transporter 4. Appl Physiol Nutr Metab 34: 481-487.

- Lafontan, M. and Langin, D. 2009. Lipolysis and lipid mobilization in human adipose tissue. Prog Lipid Res 48: 275-297.

- Lajoie, P. and Nabi, I. R. 2010. Lipid rafts, caveolae, and their endocytosis. Int Rev Cell Mol Biol 282: 135-163.

- Lamb, C. A., McCann, R. K., Stockli, J., James, D. E. and Bryant, N. J. 2010. Insulin-regulated trafficking of GLUT4 requires ubiquitination. Traffic 11: 1445-1454.

- Le Lay, S., Krief, S., Farnier, C., Lefrere, I., Le Liepvre, X., Bazin, R., Ferre, P. and Dugail, I. 2001. Cholesterol, a cell size-dependent signal that regulates glucose metabolism and gene expression in adipocytes. J Biol Chem 276: 16904-16910.

- Le Lay, S., Blouin, C. M., Hajduch, E. and Dugail, I. 2009. Filling up adipocytes with lipids. Lessons from caveolin-1 deficiency. Biochim Biophys Acta 1791: 514-518.

- Lefterova, M. I. and Lazar, M. A. 2009. New developments in adipogenesis. Trends Endocrinol Metab 20: 107-114.

- Liao, Y. and Hung, M. C. 2010. Physiological regulation of Akt activity and stability. Am J Transl Res 2: 19-42.

- Lin, Y. and Sun, Z. 2010. Current views on type 2 diabetes. J Endocrinol 204: 1-11.

- Liu, L. Z., Zhao, H. L., Zuo, J., Ho, S. K., Chan, J. C., Meng, Y., Fang, F. D. and Tong, P. C. 2006. Protein kinase Czeta mediates insulin-induced glucose transport through actin remodeling in L6 muscle cells. Mol Biol Cell 17: 2322-2330.

- Liu, L. and Pilch, P. F. 2008. A critical role of cavin (polymerase I and transcript release factor) in caveolae formation and organization. J Biol Chem 283: 4314-4322.

- Liu, L., Brown, D., McKee, M., Lebrasseur, N. K., Yang, D., Albrecht, K. H., Ravid, K. and Pilch, P. F. 2008. Deletion of Cavin/PTRF causes global loss of caveolae, dyslipidemia, and glucose intolerance. Cell Metab 8: 310-317.

- McMahon, K. A., Zajicek, H., Li, W. P., Peyton, M. J., Minna, J. D., Hernandez, V. J., Luby-Phelps, K. and Anderson, R. G. 2009. SRBC/cavin-3 is a caveolin adapter protein that regulates caveolae function. EMBO J 28: 1001-1015.

- Meshulam, T., Breen, M. R., Liu, L., Parton, R. G. and Pilch, P. F. 2011. Caveolins/caveolae protect adipocytes from fatty acid-mediated lipotoxicity. J Lipid Res.

- Nabi, I. R. 2009. Cavin fever: regulating caveolae. Nat Cell Biol 11: 789-791.

- Parton, R. G., Hanzal-Bayer, M. and Hancock, J. F. 2006. Biogenesis of caveolae: a structural model for caveolin-induced domain formation. J Cell Sci 119: 787-796.

- Parton, R. G. and Simons, K. 2007. The multiple faces of caveolae. Nat Rev Mol Cell Biol 8: 185-194.

- Robenek, H., Buers, I., Robenek, M. J., Hofnagel, O., Ruebel, A., Troyer, D. and Severs, N. J. 2011. Topography of lipid droplet-associated proteins: insights from freeze-fracture replica immunogold labeling. J Lipids 2011: 409371.

- Ros-Baro, A., Lopez-Iglesias, C., Peiro, S., Bellido, D., Palacin, M., Zorzano, A. and Camps, M. 2001. Lipid rafts are required for GLUT4 internalization in adipose cells. Proc Natl Acad Sci U S A 98: 12050-12055.

- Rowland, A. F., Fazakerley, D. J. and James, D. E. 2011. Mapping Insulin/GLUT4 Circuitry. Traffic.

- Sampson, S. R. and Cooper, D. R. 2006. Specific protein kinase C isoforms as transducers and modulators of insulin signaling. Mol Genet Metab 89: 32-47.

- Sesti, G., Federici, M., Hribal, M. L., Lauro, D., Sbraccia, P. and Lauro, R. 2001. Defects of the insulin receptor substrate (IRS) system in human metabolic disorders. FASEB J 15: 2099-2111.

- Tahir, S. A., Yang, G., Goltsov, A. A., Watanabe, M., Tabata, K., Addai, J., Fattah el, M. A., Kadmon, D. and Thompson, T. C. 2008. Tumor cell-secreted caveolin-1 has proangiogenic activities in prostate cancer. Cancer Res 68: 731-739.

- Unger, R. H. 2003. Minireview: weapons of lean body mass destruction: the role of ectopic lipids in the metabolic syndrome. Endocrinology 144: 5159-5165.

- Vinten, J., Johnsen, A. H., Roepstorff, P., Harpoth, J. and Tranum-Jensen, J. 2005. Identification of a major protein on the cytosolic face of caveolae. Biochim Biophys Acta 1717: 34-40.

- Virally, M., Blickle, J. F., Girard, J., Halimi, S., Simon, D. and Guillausseau, P. J. 2007. Type 2 diabetes mellitus: epidemiology, pathophysiology, unmet needs and therapeutical perspectives. Diabetes Metab 33: 231-244.

- Vollenweider, P., Menard, B. and Nicod, P. 2002. Insulin resistance, defective insulin receptor substrate 2-associated phosphatidylinositol-3' kinase activation, and impaired atypical protein kinase C (zeta/lambda) activation in myotubes from obese patients with impaired glucose tolerance. Diabetes 51: 1052-1059.

- Watson, R. T. and Pessin, J. E. 2001. Intracellular organization of insulin signaling and GLUT4 translocation. Recent Prog Horm Res 56: 175-193.

- Watson, R. T., Khan, A. H., Furukawa, M., Hou, J. C., Li, L., Kanzaki, M., Okada, S., Kandror, K. V. and Pessin, J. E. 2004. Entry of newly synthesized GLUT4 into the insulin-responsive storage compartment is GGA dependent. EMBO J 23: 2059-2070.

- Watson, R. T. and Pessin, J. E. 2006. Bridging the GAP between insulin signaling and GLUT4 translocation. Trends Biochem Sci 31: 215-222.

- Welsh, G. I., Hers, I., Berwick, D. C., Dell, G., Wherlock, M., Birkin, R., Leney, S. and Tavare, J. M. 2005. Role of protein kinase B in insulin-regulated glucose uptake. Biochem Soc Trans 33: 346-349.

- Williams, D., Hicks, S. W., Machamer, C. E. and Pessin, J. E. 2006. Golgin-160 is required for the Golgi membrane sorting of the insulin-responsive glucose transporter GLUT4 in adipocytes. Mol Biol Cell 17: 5346-5355.

- World Health Organization, 2011a. Obesity and overweight. Version March, 2011. http://www.who.int/mediacentre/factsheets/fs311/en/

- World Health Organization, 2011b. Diabetes. Version August, 2011. http://www.who.int/mediacentre/factsheets/fs312/en/index.html

- Yeh, J. I., Verhey, K. J. and Birnbaum, M. J. 1995. Kinetic analysis of glucose transporter trafficking in fibroblasts and adipocytes. Biochemistry 34: 15523-15531.

- Young, A. 2005. Inhibition of glucagon secretion. Adv Pharmacol 52: 151-171.

- Zaid, H., Antonescu, C. N., Randhawa, V. K. and Klip, A. 2008. Insulin action on glucose transporters through molecular switches, tracks and tethers. Biochem J 413: 201-215.